Nova Scotia's volcanic passive margin - exploration history, geology, and play concepts off southwestern Nova Scotia

Mark E. Deptuck

Canada-Nova Scotia Offshore Petroleum Board, 8th Floor TD Centre, 1791 Barrington Street, Halifax, Nova Scotia, B3J 3K9, Canada; mdeptuck@cnsopb.ns.ca

1. Introduction and scope

The crust beneath Nova Scotia's southwestern margin (box in Figure 1) is widely regarded to have formed during magmatic break-up, where multichannel seismic profiles show clear evidence for seaward dipping reflections (SDRs - Keen and Potter 1995; Shimeld 2004; Wu et al. 2006; Deptuck 2011; Louden et al. 2012; Deptuck et al. 2015), and a regional 2D refraction seismic experiment (SMART line 3; Figure 2) shows the presence of a high velocity layer interpreted as magmatically intruded or underplated crust (Dehler et al. 2004; OETR 2011). Like other magmatic margins, SDRs off southwestern Nova Scotia are interpreted as eruptive basaltic flows extruded subaerially in areas of high melt production during a break-up related magmatic event (Mutter et al. 1982; Oh et al. 1995; Keen and Potter 1995; Jackson et al. 2000). They form a northern continuation of similar features widely documented off the US Atlantic margin that generally parallel the East Coast Magnetic Anomaly (Austin et al. 1990; Oh et al. 1995; Dehler et al. 2012; Biari et al. 2017). Deptuck et al. (2015) and Deptuck and Kendell (2017) showed that SDRs continue for 220 km north of the Canada-US border, where they terminate, or show an abrupt change in width and character, at a sharp 60 km right-lateral offset in the seaward boundary of the primary salt basin (Figures 3-5). This northwest-trending right-lateral offset tracks landward along one or more synrift transfer faults or accommodation zones, and collectively these lineaments are referred to as the Yarmouth transform fault zone (YTFZ). A marked offset in salt basin position, change in salt tectonic style, and differences in crustal architecture (including the presence of clear SDRs) on either side of the YTFZ are used to distinguish the West Shelburne Subbasin to the west from the Shelburne Subbasin to the east (Deptuck and Kendell 2017; Figure 3). The latter was the focus of two recent but non-commercial exploration wells (Cheshire L-97/L-97A and Monterey Jack E-43/E-43A; Figures 1 – 3); the former has not been tested by any exploration wells, and is the focus of this study.

Beginning with a summary of the exploration history off southwestern Nova Scotia, including drilling results from the five closest wells, this report summarizes reflection seismic mapping results from both 2D and 3D data-sets along and west of the YTFZ (Figures 2, 3). These data-sets provide insight into crustal architecture along the southwestern Scotian margin, and are used to separate the study area into four distinct crustal domains (Figures 4 and 5). A description of Mesozoic seismic stratigraphy above different crustal domains follows, calibrated to available wells. These results provide insight into the break-up to early post-break-up evolution of Nova Scotia's volcanic passive margin, and the connection between crustal domain type, distribution of syntectonic strata (including primary salt), and the evolution of slope accommodation. Finally, four play concept areas along the southwestern Scotian margin are described; they mimic the distribution of crustal domains, proximal to distal changes in salt tectonic style, and water depth, and may help focus future exploration efforts.
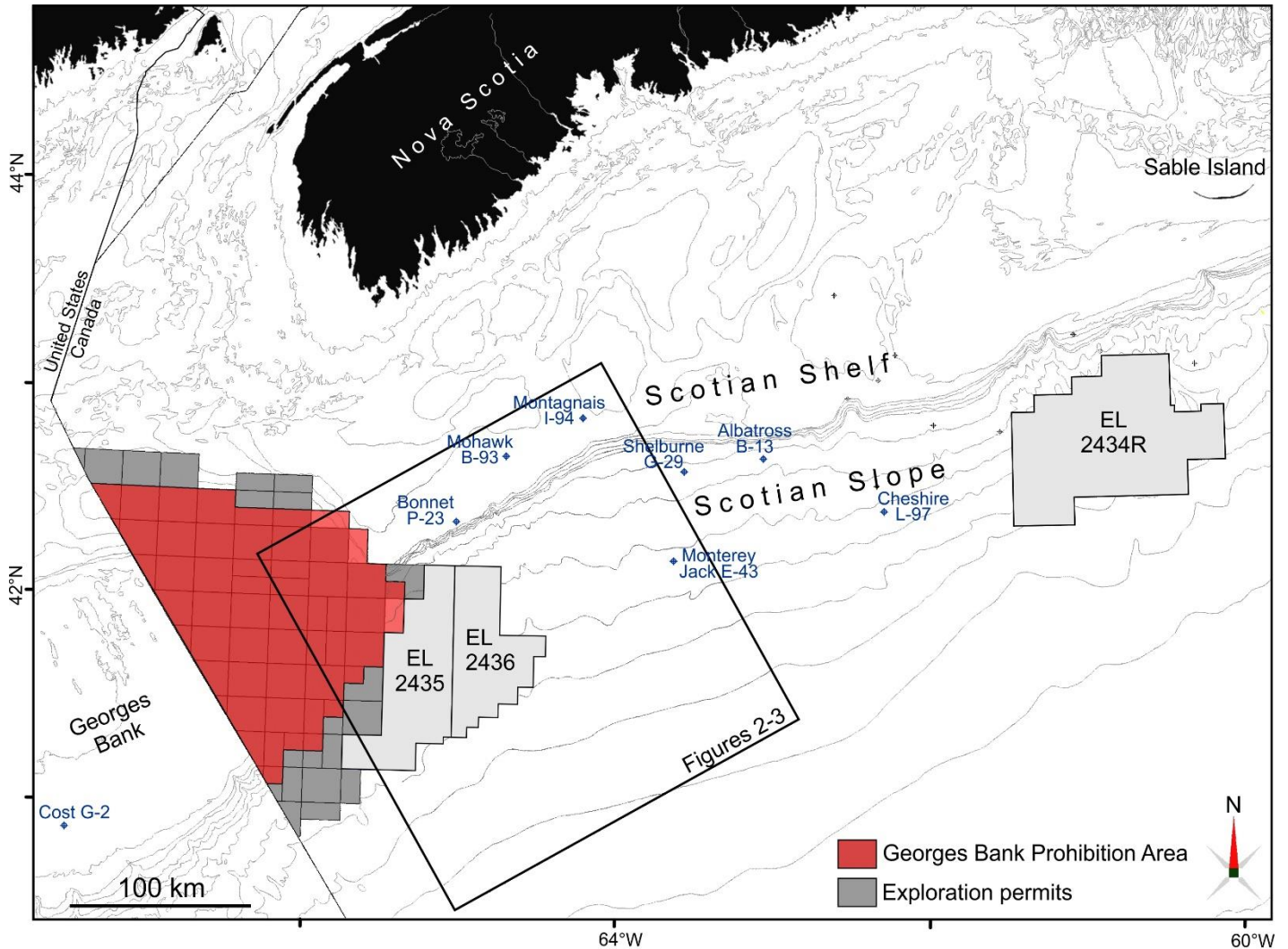
Figure 1. Map showing the location of exploration licences and key wells along the southwestern Scotian margin. Black box shows the location of the main study area.

2. Exploration history and available data

Limited coverage and quality of modern seismic data-sets, especially on the shelf, coupled with sparse well control, make the southwestern Scotian margin the most lightly explored segment of the Scotian Basin (Figures 1). Only four wells are located within the study area, providing limited stratigraphic calibration for an area covering more than >50 000 km². Exploration started on the southwestern part of the margin in the late 1960s with the acquisition of regional reflection seismic, gravity, and magnetic data-sets on the Scotian Shelf/LaHave Platform, followed by two wells in the early 1970s (Mohawk

B-93 and Montagnais I-94) and two more wells in the 1980s (Bonnet P-23 on the shelf, and Shelburne G-29 on the slope). Large basin-scale regional multi-channel seismic programs, with a line spacing of approximately 3 km, were completed on the continental slope in the late 1990s and early 2000s (Figure 2). The Barrington 3D seismic volume (CNSOPB program number NS24-P3-4E) was also acquired during this period by PanCanadian (now Ovintiv) in 2001. It covers 1795 km² on the southwestern Scotian Slope in water depths ranging from 660 to 2200 m (Figure 2). The survey is located
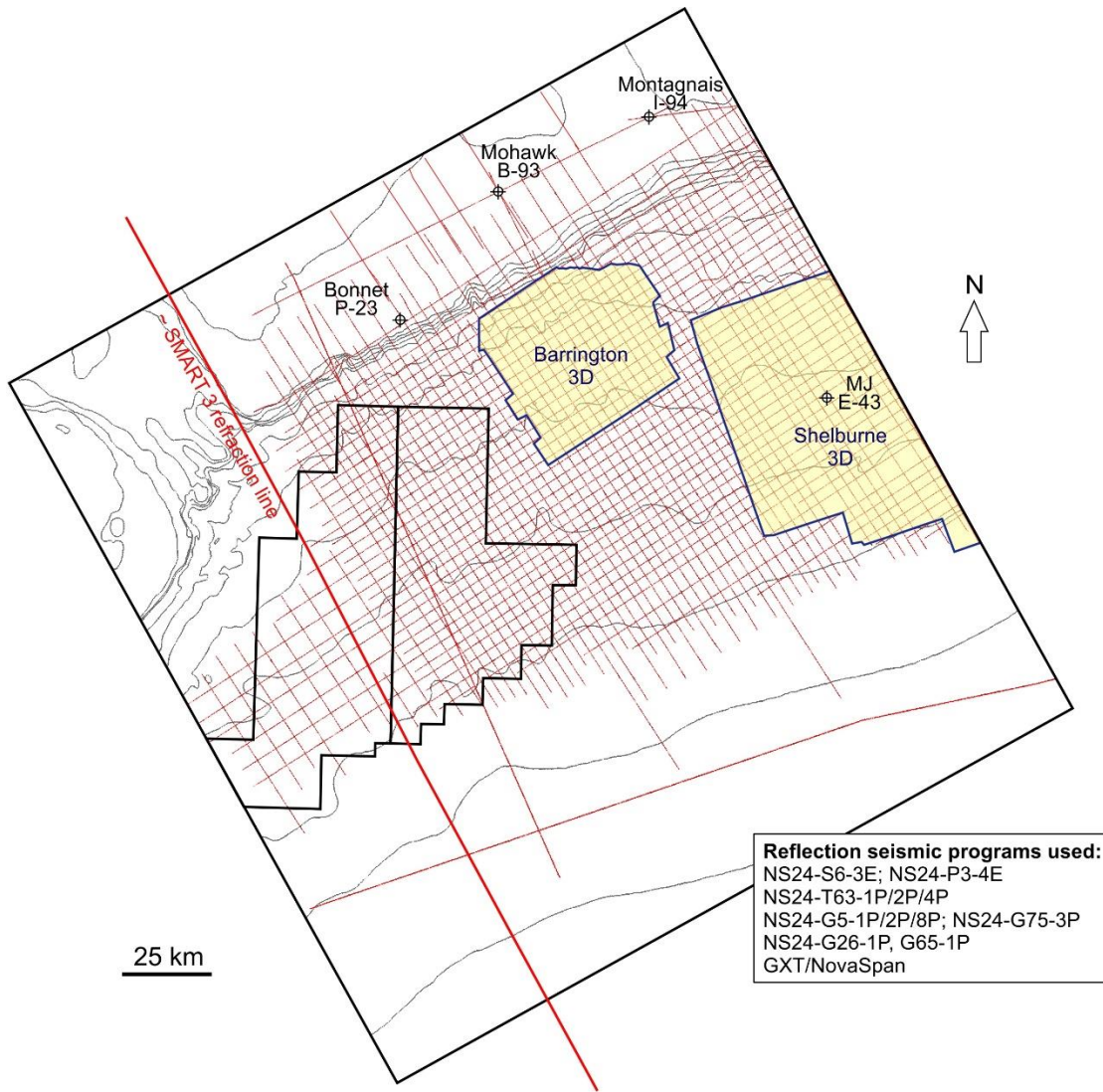
2

Figure 2. Map showing location of seismic and well data used in this study (2D seismic lines in red; 3D seismic volumes in yellow; approximate location of SMART 3 refraction experiment in bold red).

over the YTFZ that defines the boundary between the West Shelburne Subbasin and the Shelburne Subbasin (Deptuck and Kendell 2017; Figure 3), but no wells were drilled in the survey area.

Although the southwestern Scotian Slope was widely licenced by industry in the early 2000s, no additional wells were drilled until after Shell began its Shelburne Subbasin exploration campaign in 2012. The Shelburne 3D seismic volume (CNSOPB program number NS24-S6-3E) was acquired by Shell in water depths ranging from 1435 to 3460 m in

2013. This large wide azimuth survey covers approximately 10 400 km^2 and resulted in two additional slope wells – Cheshire L-97/L-97A and Monterey Jack E-43/E-43A, east of the main study area (Figures 1, 3).

In 2015, Equinor picked up the only two active parcels that cover Nova Scotia's volcanic passive margin above parts of the West Shelburne Subbasin (ELs 2435 and 2436; Figures 1, 3). No new drilling or reflection seismic acquisition has taken place yet over these parcels.

Well results

Due to substantial missing section beneath a widespread early Eocene unconformity at Montagnais I-94 (which penetrated the central uplift of an Eocene impact crater on the shelf; see Deptuck and Campbell 2012), only Mohawk B-93 (drilled in 1970) and Bonnet P-23 (drilled in 1984) calibrate Mesozoic seismic markers on the southwestern Scotian Shelf. Shelburne G-29 (drilled in 1985) and the recent Monterey Jack E-43/E-43A well (drilled in 2016) provide the only calibration of slope strata near the study area. Aside from minor gas shows in Montagnais I-94 and Bonnet P-23, there are no significant oil or gas discoveries in these wells.

The following provides, in chronological order, a summary of drilling targets and borehole results for Mohawk B-93, Montagnais I-94, Bonnet P-23, Shelburne G-29, and Monterey Jack E-43/E-43A.

Shell **Mohawk B-93** (1970) was the first well drilled on the western Scotian margin (and only the fifth drilled in the entire Scotian Basin). It was drilled in 117 m water and was designed to test a drape feature above a basement horst block inboard of the margin hingeline, above thick faulted continental crust (Figure 3). Four-way simple closure was mapped at the top of the Late Jurassic Abenaki Formation and reservoirs were expected within the Abenaki and underlying (then unnamed) fluvial siliciclastics. Aside from minor porosity present in Lower Cretaceous oolitic limestones of the "Roseway unit" (Wade and MacLean 1990) above the Abenaki Formation, the Jurassic succession was mainly composed of coarse-grained fluvial sandstones (Mohican Formation type section) with good to excellent porosity but no oil or gas shows. The well bottomed at a depth of 2124 m in a faulted basement high composed of Middle Devonian granite (Pe-Piper and Jansa 1999).

Another large basement feature was tested a few years later by the Union **Montagnais I-94** well drilled in 1974 (Figure 3). The well was spudded above the continental shelf in 113 m deep water. 2D seismic data defined a drape feature with presumed simple four-way closure on an isolated basement high. The high was surrounded by a depression and a complexly faulted outer margin. The well penetrated a thin clay-dominated Tertiary section followed by a highly mixed interval of polymictic breccias with Cretaceous to Eocene fossil assemblages (Jansa et al. 1989). Well TD was at 1644 m in highly deformed Cambro-Ordovician meta-quartzites of the Meguma Supergroup. A core through this interval shows clear shatter cones and melt rocks. Subsequent petrographic study also showed strong evidence for shock quartz, and together with the feature's structural architecture, indicates the drilling target was the central uplift of an impact crater that struck the outer continental shelf at ~50.5 Ma (Early Eocene) (Jansa and Pe-Piper 1987). A shallow minor gas show was found at 377.6-383.7 m in unconsolidated Quaternary gravels but was not tested. See Jansa and Pe-Piper (1987), Jansa et al. (1989), Deptuck (2011), and Deptuck and Campbell (2012) for a more detailed description of this marine-target impact event.

Petro-Canada **Bonnet P-23** (1984) is the western-most well in the Scotian Basin (Figure 1). It was drilled to test a large (~70 km^2), elongate, fault-bounded rollover structure located about 6 km inboard of the highly faulted Jurassic carbonate bank edge in 133.5 m deep water. Closure was mapped at the interpreted Late Jurassic Mohawk seismic horizon, with its fluvial sandstones the primary reservoir target. About 1762 m of Tertiary mudstones were encountered above a major unconformity that cuts down through the Cretaceous section leaving a ~300 m interval of Lower Cretaceous carbonates of the informal "Roseway unit" (Wade and MacLean 1990; Weston
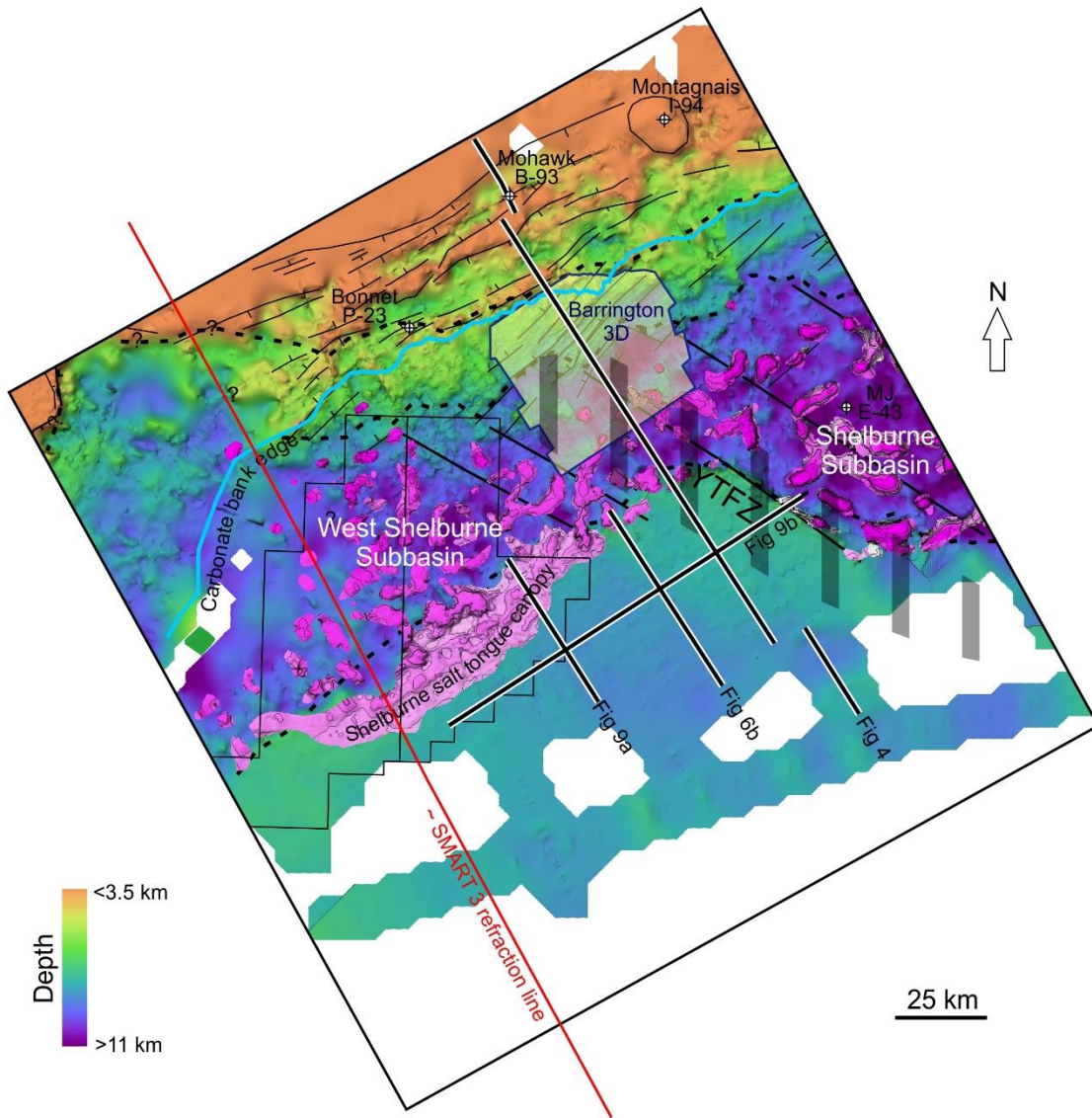
Figure 3. Top basement structure map, southwestern Scotian margin. Salt diapirs shown in pink. Line locations in black with white shadow. Barrington 3D volume shown in yellow. Boundaries between crustal domains shown in black dashed lines, and carbonate bank edge shown in blue. YTFZ = Yarmouth transform fault zone (hatchered area). Approximate location of SMART 3 refraction line shown in red.

et al. 2012). This was followed by the entire Middle to Late Jurassic Abenaki Formation. The carbonates are dominantly oolitic limestones and minor dolomites having occasional fair (inter-oolitic), to very good (intercrystalline dolomitic) porosity in lagoonal facies mudstones. No reef-related facies were present. The well TD was at 4336 m in Bathonian dolomites, but the basal 450 m of the well section was not accurately evaluated due to extensive lost circulation zones, incomplete mud-

gas logging, lost mud and sample returns, etc. that may be the result of enhanced porosity intervals or the presence of several large faults in this section. Four peaks on the mud-gas log under 100 TGU were encountered here and minor oil staining in two samples but no tests done. Expected coeval Mohawk or Mohican sandstones were not present.

The fourth well, **Shelburne G-29**, was drilled by Petro-Canada in 1985. It was spudded on the continental slope in 1153.5 m deep water. The

primary target was an interpreted turbidite fan of Paleocene to possibly Maastrichtian age. The secondary target was an underlying southwest-plunging structural nose of the interpreted Jurassic Abenaki carbonate margin (Middle Jurassic Scatarie Member) and dolomitic Iroquois Formation above a salt pillow. Modern seismic data now indicates a prominent basement fault block produced this structural high, and the well was located seaward of the Jurassic carbonate bank edge. A few minor sandstones with scattered fair to very good porosity were encountered in upper Cenozoic strata. In the target interval (later confirmed to be the Late Cretaceous Wyandot and Dawson Canyon formations; Wade and MacLean 1990), the suspected turbidite fan was found to be a succession of limestones, marls and shales, with the remaining interval being almost entirely shale. The well penetrated the top of the Abenaki Formation (Baccaro Member) and a core was attempted. However, after cutting 14.5 m of core the drill string became stuck while pulling out of the hole and following unsuccessful attempts to retrieve it the well was abandoned at a TD of 4005.5 m. No reservoirs or hydrocarbon shows were present.

The fifth well, **Monterey Jack E-43/E-43A,** was drilled by Shell in 2016 in 2118 m of water on the continental slope, above the Shelburne Subbasin. It, along with Cheshire L-97/L-97A located roughly 120 km further east, are the first wells to be drilled in more than 30 years along the southwestern Scotian margin. Monterey Jack E-43/E-43A targeted a subtle four-way dip closure produced in folded Jurassic to Lower Cretaceous strata on the slope. The well targeted an interpreted Lower Cretaceous turbidite reservoir interval within a salt withdrawal minibasin that is surrounded by expelled salt bodies (Figure 3). The structure is technically a salt-cored fold, but little salt now remains along the primary salt weld; the fold instead appears to have formed as a compressional response to Cretaceous reactive

diapirism and detachment of cover strata above the primary salt layer (or its weld). The fold also appears to have localized above the angular edge of a faulted basement block within hyperextended crust, along which the primary salt layer welded out (see later discussion). No reservoirs were encountered in the target interval, which instead was dominated by claystones and marls, and no hydrocarbon shows were present. Well TD was in Callovian limestone, claystone and marl. Refer to the CNSOPB SCOPE Atlas (2020) for a more detailed account of the well results.

3. Geological Setting

Crustal architecture

Figure 3 shows the structure of the top basement surface, interpreted basement-involved faults, and location of salt diapirs expelled from a primary salt basin. The top crust surface deepens from roughly 2 km on the platform (e.g. Mohawk B-93, encountered Devonian granites at a depth of 2.11 km in the landward parts of Figure 3; see Pe-Piper and Jansa 1999) to more than 9 km deep beneath the salt basin further seaward. A representative transect across the shelf and slope off southwestern Nova Scotia shows the overall margin structure, including the location of rift basins, primary salt layer, and SDRs (Figure 4). The landward and seaward M markers at the base of the crust (M_L and M_S markers, respectively), Top Paleozoic Basement (TPB), and the Top SDR marker, combined with a number of additional internal crustal markers and basement-involved faults, constrain crustal thickness and architecture along the southwestern Scotian margin (Deptuck 2018).

Despite the presence of SDRs along the seaward segment of Figure 4 and the dominance of landward dipping faults – both common characteristics of volcanic passive margins (e.g. Planke et al. 2000; Franke 2000; Pindell et al. 2014; Geoffroy et al. 2015; McDermott et al. 2015; Reuber et al. 2019) –
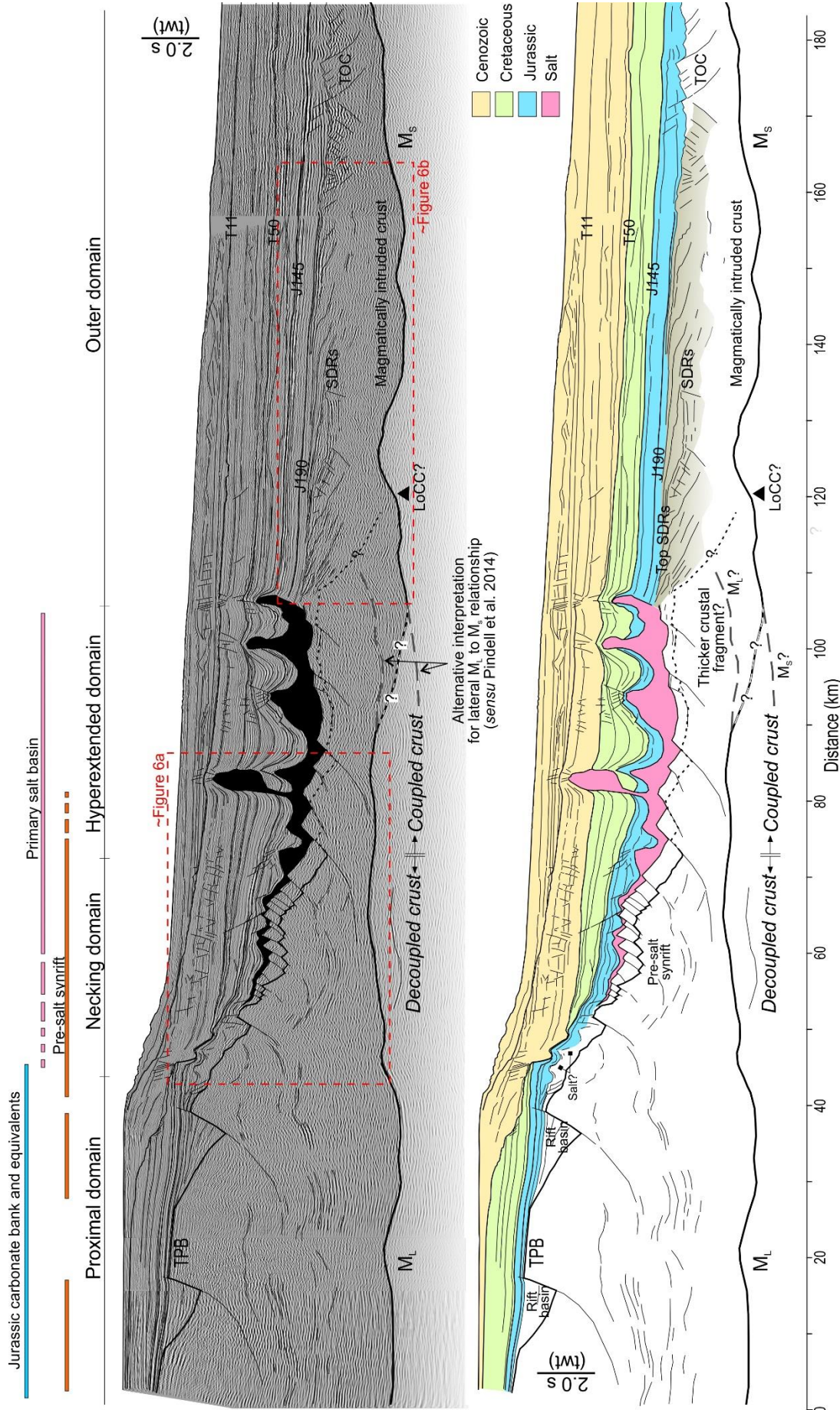
Figure 4. Representative composite seismic profile across the southwestern Scotian Shelf and Slope. See Figure 3 and 5 for location. Figures 6a and 6b are along strike from Figure 4. An alternative interpretation for the lateral relationship between the M_L and M_s markers is also shown. Sub-continental mantle lithosphere separates the two markers in the alternate scenario, where the M_s marker would correspond to an oceanic Moho (see Pindell et al. 2014). Note that the water column was depth converted, but the section below the seabed is in travel time. LoCC = limit of continental crust; SDRs = seaward dipping reflections; TPB = top Paleozoic basement; TOC = transition to oceanic crust

Figure 5. Crustal domains along the southwestern Scotian margin. Crustal thickness based on 6.5 km/s crustal velocity. Note that the SMART 3 refraction profile described by Dehler et al. (2004) is located just west of where the M_L marker is present in existing reflection profiles. Salt diapirs in pink. Transfer faults in red. YTFZ = Yarmouth transform fault zone (red hachured). Carbonate bank edge in blue. VB = volcanic belt

the overall crustal structure also shares a number of similarities with non-magmatic margins. The presence of mid-crustal shear zones separating brittle upper crust from ductile middle to lower crust, clear syntectonic successions including rift basins and an overlying synrift primary salt layer, and most importantly the absence of widespread extrusive magmatism above the necking domain, are all characteristics shared by magma-poor margins (e.g. Peron-Pinvidic et al. 2013; Sutra et al. 2013; Chenin et al. 2017). As such, a hybrid of criteria borrowed from both magma-poor and volcanic passive margin studies are used here to separate the southwest Scotian margin into different crustal domains (Figures 4 and 5). In particular, the degree of parallelism between the top and base of the crust (Peron-Pinvidic et al. 2013; Chenin et al. 2017), is relatively straight-forward to define in the study area.

8

Proximal domain

The thickest crust in the study area – corresponding to the *proximal domain* in Figure 5 – is found along the outer part of the LaHave Platform. Using a single-layer average crustal velocity of 6.5 km/s (a necessary oversimplification given the dearth of available crustal velocity constraints), proximal domain crust in Figure 4 is 20 to 30 km thick, with roughly parallel top and base surfaces (Figure 5). Clear decoupling of brittle upper crust from more ductile middle to lower crust took place across mid-crustal shear zones. Likewise, the top of the crust is offset along a series of mainly landward dipping border fault that sole into these mid-crustal shear zones, and a number of thick, generally poorly imaged half-graben style rift basins are preserved above proximal domain crust (Welsink et al. 1989). They are similar to rift basins described by Deptuck and Altheim (2018) on the central Lahave Platform. No wells calibrate their fill.

Necking domain

Decoupled crust continues into the relatively narrow *necking domain* defined by the abrupt seaward taper in crustal thickness as the top and base crust surfaces converge seaward of the margin hinge (Figures 4 and 5). The crust thins from 20 km to just 9 km thick over distances of about 25 km. The seaward boundary of the necking domain coincides closely with the *coupling point* (see Peron-Pinvidic et al. 2013), where basement faults sole near the base of the crust, rather than along mid-crustal shear zones (Figure 4). In plan view, this boundary is irregular, comprising a series of right-stepping offsets (Figure 5). Layered pre-salt stratigraphic successions of unknown composition veneer faulted basement in the necking domain (e.g. Figure 6a), but the succession is thinner than equivalent rocks preserved in half-graben style rift basins further landward. One very bright amplitude reflection, which locally cross-cuts other pre-salt seismic markers, may correspond to an igneous intrusion in

the necking domain, but there is no evidence for widespread "hinge zone" or "inner" SDRs here of the kind described by Oh et al. (1995); McDermott et al (2015), Paton et al. (2017), or Reuber et al. (2019).

Hyperextended domain

Further seaward, thinner crust of the *hyperextended domain* is 4 to 9 km thick (Figure 5). Brittle upper and ductile middle to lower crust cannot be distinguished. The subsalt seismic character is generally more reflective and incoherent here, produced by either a thin reflective pre-salt succession or a more reflective top basement surface associated with coupled crust. An increase in pre-salt magmatic additions to the crust or the overlying veneer of early synrift strata, could explain this change. However, poor seismic imaging here decreases interpretation confidence; this is at least partly a consequence of the increasing complexity of overlying salt bodies here.

The primary salt basin spans both the necking and hyperextended domains, and may even locally extend into poorly imaged rift basins perched above proximal domain crust (Deptuck et al. 2015). The tallest generally vertically expelled salt bodies, however, are limited mainly to areas underpinned by hyperextended crust, implying that the primary salt basin was thickest here (with salt pillows and rollers being the dominant salt bodies above thicker crust further landward). Crustal faults, in addition to offsetting the layered pre-salt series, clearly displace the base and in some cases even the top of the transparent Late Triassic or earliest Jurassic interval of deformed evaporates (Figure 6a). This implies that salt accumulated during active lithospheric extension (i.e. is syntectonic) and falls into the late syn-stretching to syn-thinning (or syn-hyper-extension) classification of Rowan (2014) or middle to late synrift salt of Allen and Beaumont (2015) and Allen et al. (2019).
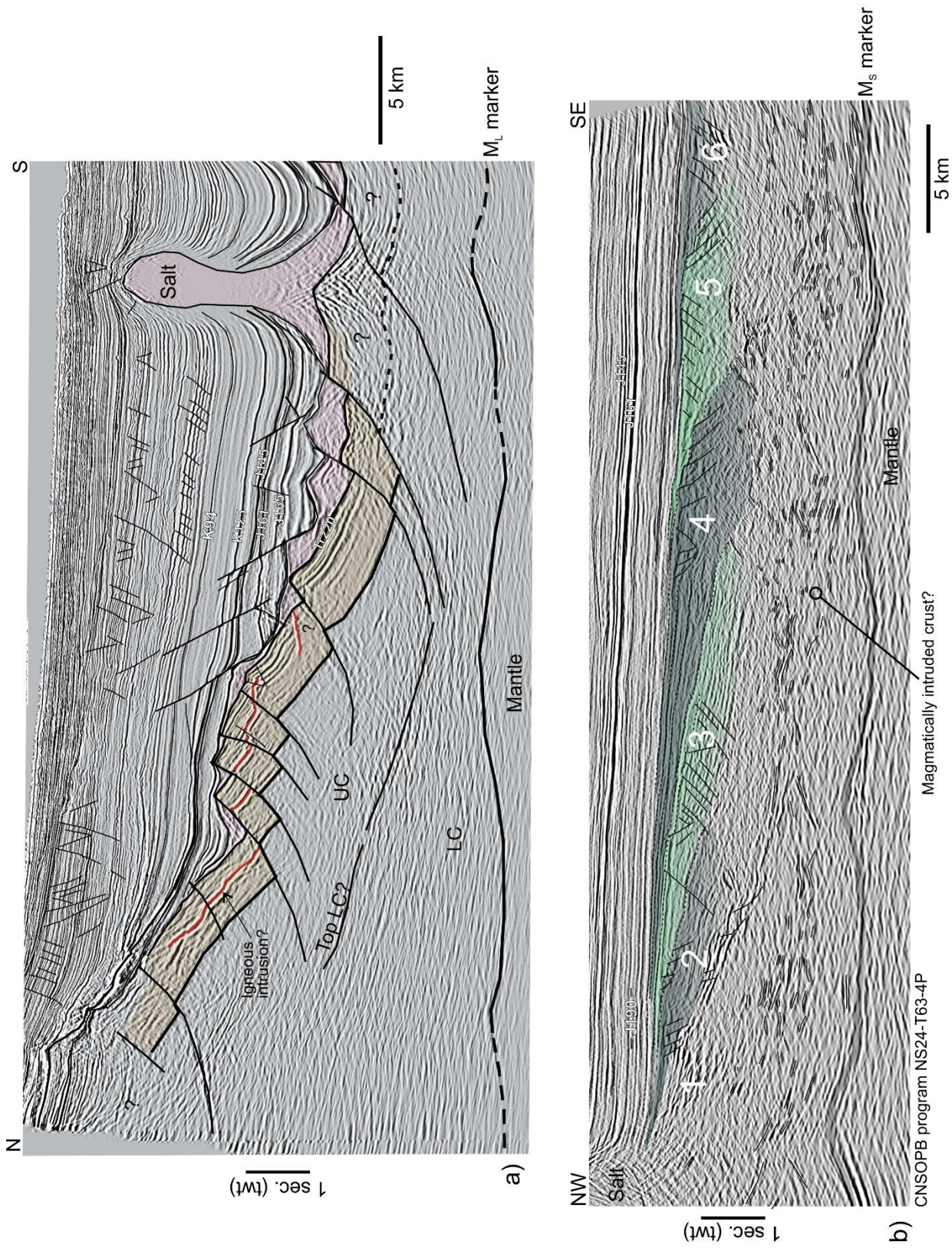
9

Figure 6. a) Dip section through Barrington 3D volume across the necking to hyperextended domain. The thickness of pre-salt synrift strata below the right side of the figure is uncertain. b) Dip section through outer domain crust showing succession of seaward dipping reflections that young towards the right. See Figure 3 for location. LC = lower crust; UC = upper crust

Together, the coincidence of a shallow reflection Moho beneath the primary salt basin ('Moho high' of Deptuck 2018), the location of overlying hyperextended crust, and the distribution of prominent salt structures, suggests that the thickest parts of the primary salt basin developed where the most rift-related accommodation space was available during late stage crustal thinning (coinciding with the thinnest crust). The TPB surface cannot be correlated seaward of the primary salt basin. It probably underlies the complex succession of reflective markers that make up the SDR series, but it is unclear how far seaward under the SDRs continental crust continues. A thicker fragment of continental crust (or altered/magmatically intruded continental crust) may directly underlie the seaward edge of the salt basin in Figure 4, and if so, the limit of continental crust (LoCC; McDermott et al. 2015; Reuber et al. 2019) is notionally placed beneath the landward most SDRs where a relatively bright base SDR marker converges towards the base of the crust. The ~1.5 km basement step typically observed at the seaward edge of the primary salt basin (Deptuck and Kendell 2017; see Figure 3), could be the combined result of a thicker fragment of continental crustal here and later vertical build-up of younger volcanic material above it. An alternate interpretation for the lateral relationship between the M_L and M_S markers is also possible, and would reduce the need for a thicker continental crustal fragment here (Figure 4).

Outer domain

The *outer domain,* located seaward of the primary salt basin in Figure 5, corresponds to the region of magmatically intruded or underplated crust identified along strike in the SMART 3 refraction experiment by Dehler et al. (2004). The M_S marker is a strong undulating reflection beneath outer domain crust, interpreted as a reflection Moho (oceanic?). Together with the "Top SDR" surfa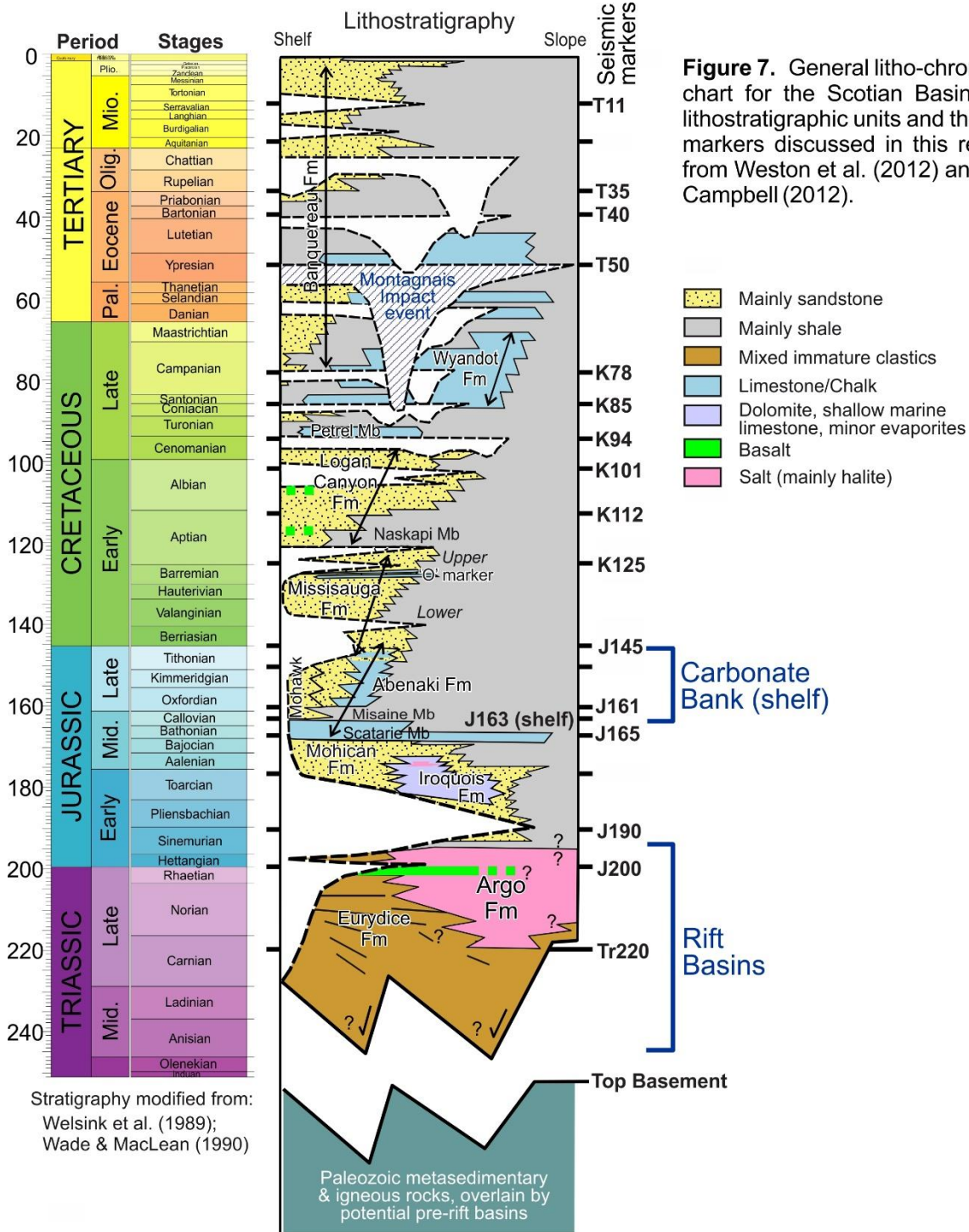ce correlated above the 60 km wide reflective and complexly layered succession of SDRs, crust of the outer domain is generally tabular, with roughly parallel top and base surfaces (except where the M_S marker is locally rugose, as in Figure 4). On the SMART 3 refraction line this crust is 10 km thick (Dehler et al. 2004), noticeably thicker than the crust immediately landward. Partly a consequence of the volcanic additions that veneer the crust, the increased thickness could also be due to magmatic addition associated with underplating (Dehler et al. 2004). The overlying SDRs have been separated into 5 or 6 distinct volcanic bands, each corresponding to a seaward dipping and thickening wedge of interpreted volcanic or volcaniclastic material that developed during mainly southeast-directed accretion (Figure 6b). Clusters of faults, subtle changes in seismic stratigraphy, or periods of aggradation distinguish successive volcanic bands.

The SDR series is increasingly offset across seaward dipping faults in the seaward part of Figure 4, where the top crust and base crust (M_S marker) surfaces once again converge, with crust thinning to as little as 7 km. Although only three dip profiles and one strike profile extend this far seaward on the southwestern Scotian margin, all show a transition to this more heavily faulted crust, with internal layering that resembles the reflectivity of the SDRs, but with more arbitrary but generally landward dip directions (Figure 5). As such, the seaward most crust in Figure 3 is inferred to be transitional crust between SDRs and true Penrose-type oceanic crust accreted along the mid- Atlantic ridge after the outer margin foundered. Some rotated blocks in this crust are structurally elevated and onlapped by pre-J165 strata seaward of the primary salt basin.

Post-salt stratigraphic evolution

Stratigraphy above proximal, necking, and hyperextended domain crust

Mesozoic postrift cover strata are thinnest above the outer LaHave Platform where relatively little thermal subsidence took place. Here, a prominent

Figure 7. General litho-chronostratigraphic chart for the Scotian Basin, showing the lithostratigraphic units and the main seismic markers discussed in this report. Adapted from Weston et al. (2012) and Deptuck and Campbell (2012).

Callovian to Tithonian carbonate bank (Abenaki Formation; Wade and MacLean 1990; Figure 7) aggraded above thick crust of the proximal domain and its associated rift basins. Carbonates of the Abenaki Formation were calibrated at Bonnet P-23, with the next closest well located more than 150 km east (Albatross B-13; see Figure 1). Its base corresponds to the J163 seismic marker produced by a reflection between condensed clastics of the Misaine Member and widespread platformal oolitic carbonates of the underlying Scatarie Member, both in the lower part of the Abenaki Formation (Wade and MacLean 1990; Weston et al. 2012). As shown by Mohawk B-93, the carbonate-dominated platform can pass abruptly landward into a clastic-dominated equivalent succession over distances of less than 20 km. On seismic profiles, thin locally-developed intervals of prograding seismic facies both predate the J163 marker and form isolated forced regressions just above it, or in lieu of it (e.g. seaward of Mohawk B-93, see figure 2.15 of Deptuck et al. 2015). This suggests there were periods when small Jurassic deltas delivered more clastic-prone sediment to the proto-continental slope before and during the early development of the carbonate bank (see also OERA 2015).

By the end of the Jurassic, a well-defined carbonate bank edge developed along the margin hinge that separates proximal from necking domain crust (Deptuck and Altheim 2018) (Figure 5). Seaward of it, a steep carbonate foreslope developed above more rapidly subsiding basement of the necking domain. In addition to establishing where platform versus slope carbonates were deposited, increased thermal subsidence of thinner crust seaward of the proximal domain is responsible for increasing the gradient of the proto-continental slope. The Barrington 3D survey, which crosses the necking domain and extends above hyperextended crust, affords a clearer picture of how the slope evolved. Here, the J163 marker diverges into two separate

surfaces (the Late Bathonian J165 marker and the Late Callovian J161 marker) where the Middle Jurassic succession is more expanded (calibrated at Cheshire L-97/L-97A located 111 km east of Monterey Jack E-43/E-43A; CNSOPB SCOPE Atlas 2020). Combined with the end Jurassic J145 marker, these surfaces track important changes in paleo-bathymetry on the slope as the carbonate bank aggraded on the platform (Figure 8).

An amplitude extraction from the J165 marker in the Barrington 3D survey shows the oldest down-slope trending erosional features recognized beneath the modern continental slope (Figure 8a). These somewhat disorganized channels, with discon-tinuous sinuous planform geometries, may record the early development of the proto-continental slope as the distal necking domain subsided after break-up. These disorganized channels pass up-section into wider, more sharply defined, curvi-linear erosional channels/canyons at the J161 marker (Figure 8b). Their heads produce a subtle dendritic pattern approaching the platform, suggesting a shelf edge had developed near the margin hinge by this time. J161 channels in turn pass up-section into prominent dendritic canyon heads at the J145 marker, eroding the steep carbonate foreslope immediately seaward of the erosionally scalloped bank edge (Figure 8c). The canyon heads, arranged along strike into an overlapping networks of converging gullies, merge downslope into a number of more widely spaced trunk channels/canyons that re-occupied underlying J161 channels. The temporal change in Jurassic channel geomorphology is consistent with the progressive steepening of the proto-continental slope from the J165 to J161 to J145 markers. The increasing gradient was probably prompted by a combination of seaward increasing thermal subsidence and landward aggradation of shelf carbonates above the outer platform.
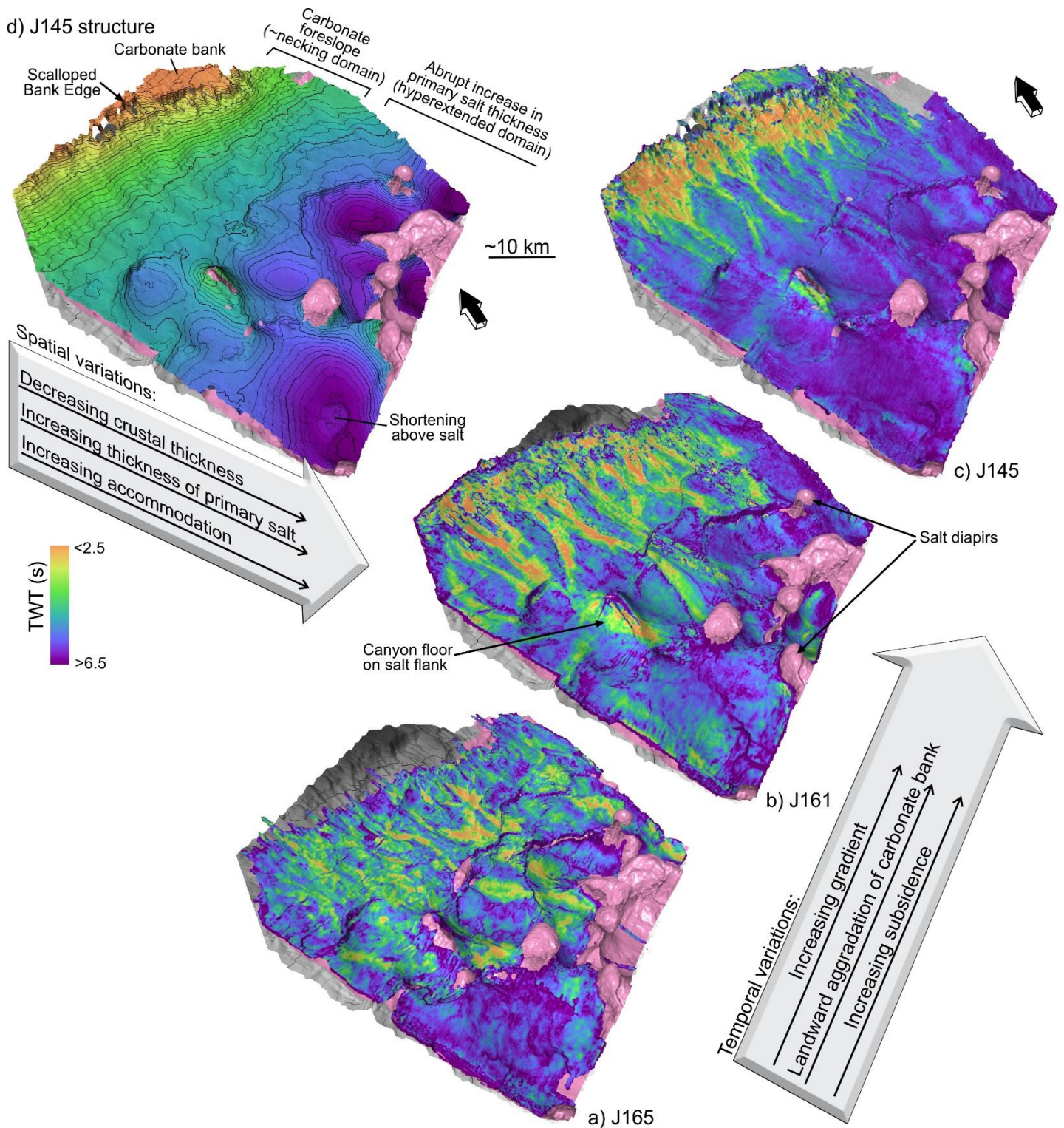
Figure 8. RMS amplitude extractions from the a) J165, b) J161, and c) J145 markers in the Barrington 3D seismic volume, showing the progressive development of early postrift channels on the proto-Scotian Slope as necking to hyperextended crustal domains steepened in response to postrift thermal subsidence. d) Time-structure map along the J145 marker showing the heavily eroded and scalloped carbonate bank edge with steeper carbonate foreslope seaward, and rising salt diapirs further seaward still. Contour interval is 100 ms (twt). See Figure 3 for location and text for details.

The carbonate system established in the Jurassic had a lasting influence as the margin continued to develop in the Cretaceous and into the Paleogene. Beginning with a mixed carbonate and clastic depositional system in the early Cretaceous (Roseway unit; Wade and MacLean 1990; Moscardelli et al. 2019), followed by more clastic dominated systems in the mid-Cretaceous, and then condensed chalk and marl dominated intervals in the Turonian through Eocene (e.g. Fensome et al. 2008), successive unconformities localized erosion above the fossil carbonate bank edge. The result is generally thin preservation of Cretaceous to early Paleogene strata above the outer parts carbonate platform and steep carbonate foreslope (e.g. figure 7b of Deptuck and Campbell 2012). This is mainly the product of superimposing clastic depositional systems above a steeper carbonate slope profile (to produce an out-of-grade slope *sensu* Ross et al. 1994; Prather 2020), with successive unconformities attempting to regrade the carbonate slope to achieve a lower gradient more typical of clastic depositional systems.

At least six Cretaceous to early Paleogene erosive surfaces converge upslope in the landward parts of the Barrington 3D survey, approaching the Jurassic bank edge (see CNSOPB SCOPE Atlas 2020). Geomorphologies along these erosive surfaces vary from narrow dendritic channels that converge downslope into wider linear trunk channels or canyons, to very wide linear incisions (> 5 km) that removed broad swaths of slope strata; all acted as conduits that bypassed sediment gravity flows further seaward, but the extent to which each was connected to a fluvial-deltaic sediment delivery system is not known. Erosive surfaces are commonly more difficult to correlate where active subsidence took place in salt withdrawal minibasins above hyper-extended crust (mainly above the thickest parts of the primary salt basin, e.g. Figure 8d), but a number of erosive surfaces also continue seaward
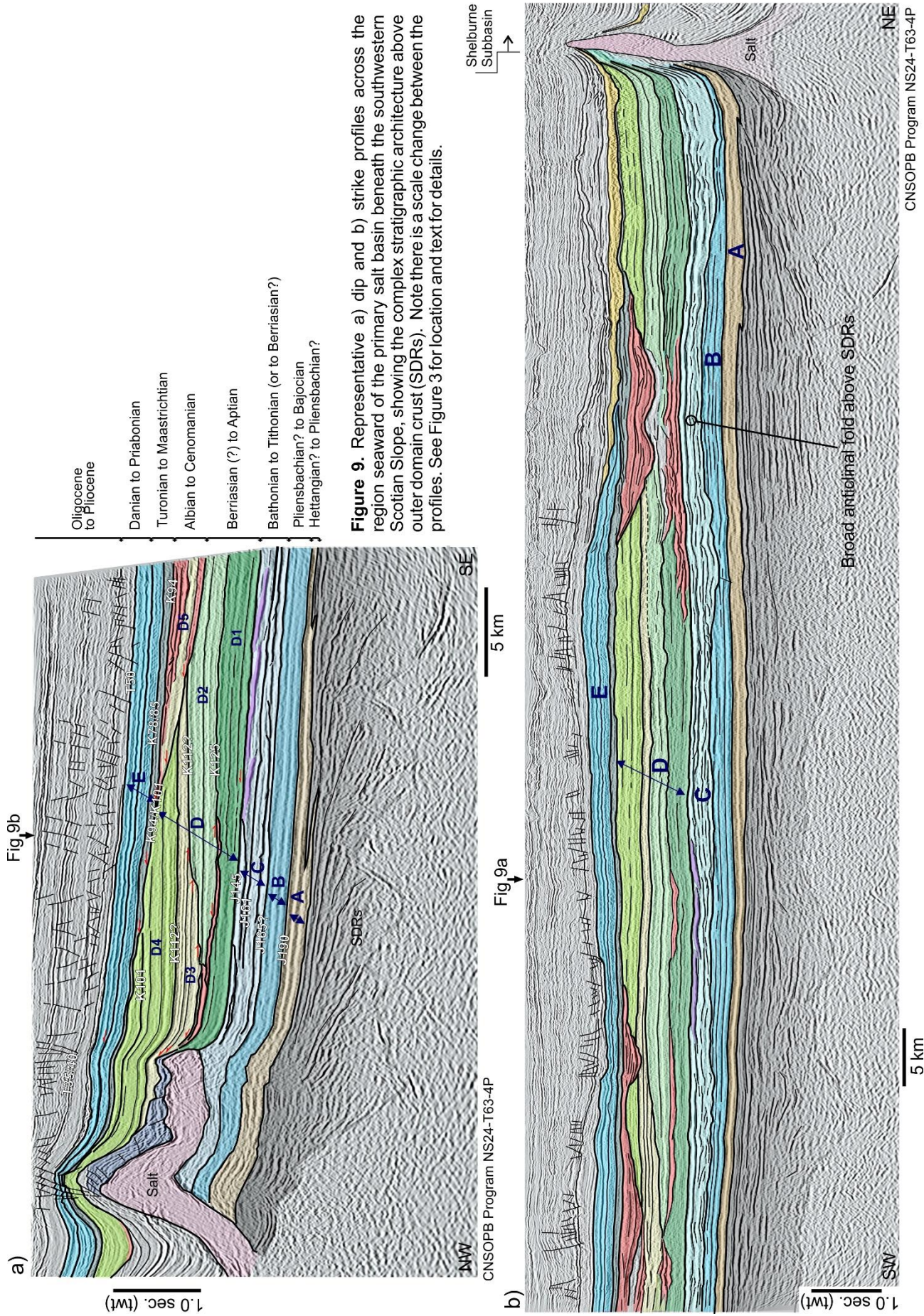
of the primary salt basin, indicating that the largest sediment gravity flows continued to transit the seabed beyond the rising diapirs and intervening minibasins further landward.

The final attempts to regrade the inherited carbonate slope profile took place in the early Paleogene, when the widespread Early Eocene T50 unconformity (in particular) associated with the Montagnais impact event produced widespread erosion across the outer shelf, slope, and abyssal plain (Deptuck and Campbell 2012). An associated mass transport deposit was correlated for more than 500 km seaward of the underlying carbonate bank edge, where it ultimately pinches out along the flanks of the New England Seamounts (Deptuck and Campbell 2012).

Younger Cenozoic intervals aggraded and prograded above the carbonate bank and its sharply defined bank edge, filling in the widespread Montagnais erosive surface on the shelf and upper slope (Campbell et al. 2015). Further seaward, a combination of down-slope gravity-flow-dominated processes (generating mass transport deposits, canyons, and migrating submarine channels), and cross-slope bottom-current-dominated processes (generating contour-ite drifts, sediment waves, and along-slope scours) produced a complex arrangement of Oligocene to Pliocene seismic facies (Campbell and Deptuck 2012; Campbell et al. 2015; Campbell and Mosher 2015) (Figure 4).

Stratigraphy above outer domain crust
The ~3-6 km grid of 2D seismic profiles seaward of the primary salt basin (and allochthonous salt bodies expelled from it) provides a rare window into Mesozoic seismic stratigraphy deposited without the effects from salt-related deformation. The Jurassic and Cretaceous stratigraphic record above outer domain crust here is complex and interesting, comprising a number of erosional and depositional elements within or bounding aggrading, migrating

Figure 9. Representative a) dip and b) strike profiles across the region seaward of the primary salt basin beneath the southwestern Scotian Slope, showing the complex stratigraphic architecture above outer domain crust (SDRs). Note there is a scale change between the profiles. See Figure 3 for location and text for details.

Oligocene to Pliocene

Danian to Priabonian

Turonian to Maastrichtian

Albian to Cenomanian

Berriasian (?) to Aptian

Bathonian to Tithonian (or to Berriasian?)

Pliensbachian? to Bajocian
Hettangian? to Pliensbachian?

or abruptly shifting depocenters (Figure 9). As the SDRs at the base of the interval constrain both (i) latest rift evolution (transition to break-up) and (ii) paleo-bathymetry (SDRs are interpreted to form from volcanic flows on land), vertical changes in the seismic facies above SDRs record the final break-up to early post-break-up evolution of the outer domain, as well as the transition from terrestrial to deep marine depositional settings. Although there is no well control in this setting, Figure 9 records several distinct periods of sedimentation – labelled (A) through (E) – providing a clearer picture about the stratigraphic evolution above outer domain crust.

Immediately above or inter-fingering with the SDRs is a seaward-thinning wedge of low to moderate amplitude reflections (**A**) that pinch out above the youngest volcanic wedges (Figure 9a). Two widely distributed moderate amplitude soft loops (troughs) define its top (potential source rocks?). That Unit A thickens landward implies subsidence was focused landward of the SDRS during and shortly after SDR-emplacement, perhaps a continuation of subsidence that lead to earlier deposition of the primary salt basin above hyperextended crust (e.g. a sag basin above the primary salt basin?). Unit A could record the accumulation of shallow marine deposits in a restricted shallow sea located landward of the topographically elevated succession of terrestrial SDRs, or could alternately be composed of volcaniclastics that aggraded off-axis to the elevated volcanic wedges.

Unit A passes up-section into a low amplitude mainly layer-cake draping succession that, except for broad scours that erode it from above and seaward thinning onto distal rotated basement blocks (seaward of the SDRs), shows little spatial variation in thickness (**B**). Reflection frequency is generally low, and layered successions on some strike profiles pass laterally into reflection free intervals of uncertain origin. The absence of onlap surfaces in layered intervals implies a low energy environment with passive sedimentation (marls and mudstones?), though more transparent intervals could represent localized Lower Jurassic shallow water carbonate build-ups deposited during the earliest stages of post-SDR thermal subsidence.

Unit B passes up section across a poorly defined unconformity or a series of unconformities, into an interval with sharply higher reflection amplitude (**C**; Figures 7, 8). The J165 surface described landward is located either at the base of (C) or in its lower parts; the sharply defined top of (C) corresponds to the J145 marker (tied to Monterey Jack E-43/E-43A; CNSOPB SCOPE Atlas 2020). Elevated reflectivity of Unit C is likely caused by a combination of increasing carbonate content of these sediments (associated with aggradation of the Abenaki carbonate bank) and complex sediment transport across a thermally subsiding continental margin (e.g. Figure 8). Reflection complexity also increases sharply in Unit C, with a number of very bright discontinuous reflections arranged in seemingly disorganized mounded, lensing, and erosional geometries (scours or channels). This could be caused by intercalated clastics supplied by hinge zone deltas before or during early development of the Abaneki carbonate bank (Deptuck 2011), or the accumulation of resedimented carbonates in calci-clastic submarine fans.

This interval also contains a series of well-organized shingled very bright amplitude reflections that stack/prograde towards the southeast. They can be correlated along-strike for tens of kilometers where they form linear bands that resemble the prograding Jurassic oolitic shoals described by Hanford and Baria (2007) in the Smackover Formation, in the Gulf Coast of the United States. That these shingled reflections overlie the J165 surface, however, implies water depths were probably too deep at this time for oolitic shoals. These shingled reflections may instead have formed during the migration of
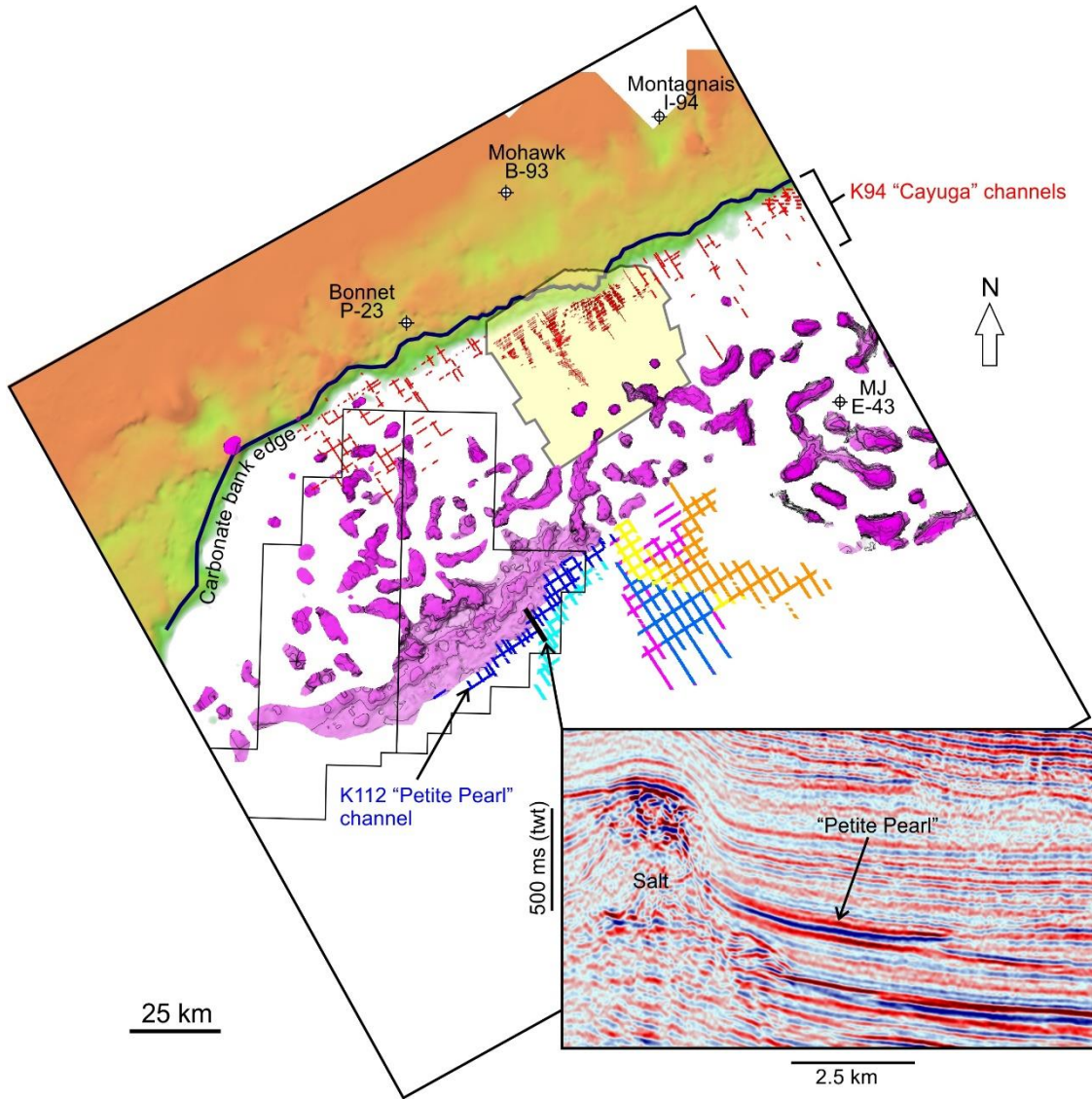
Figure 10. Map showing the location amplitude anomalies associated with the K94 "Cayuga" channel systems that onlap the steep carbonate foreslope. Also shown are a number of other Lower to mid Cretaceous channel corridors mapped seaward of the primary salt basin, above outer domain crust. Inset shows the "Petite Pearl" anomaly that tracks along the Shelburne salt tongue canopy.

broad northeast-trending turbidite channels supplied from the northwest as clastic deltas prograded across Georges Bank above the J163 marker (OERA 2015; Deptuck et al. 2015), or they could mark the onset of Middle Jurassic slope parallel (SW or NE directed) ocean currents that reworked underlying deepwater (or even shallower water) carbonates, clastics, or both.

Abruptly overlying the J145 marker is a complex mixed-amplitude Lower to mid Cretaceous interval containing the K125, K112, K101 and K94 markers (**D**; Figures 7, 9), correlated into Monterey Jack E-43/E-43A with a moderate to high degree of confidence (CNSOPB SCOPE Atlas 2020). Except for sharply defined thins caused by canyon incision along the overlying K101 erosional surface, Unit D
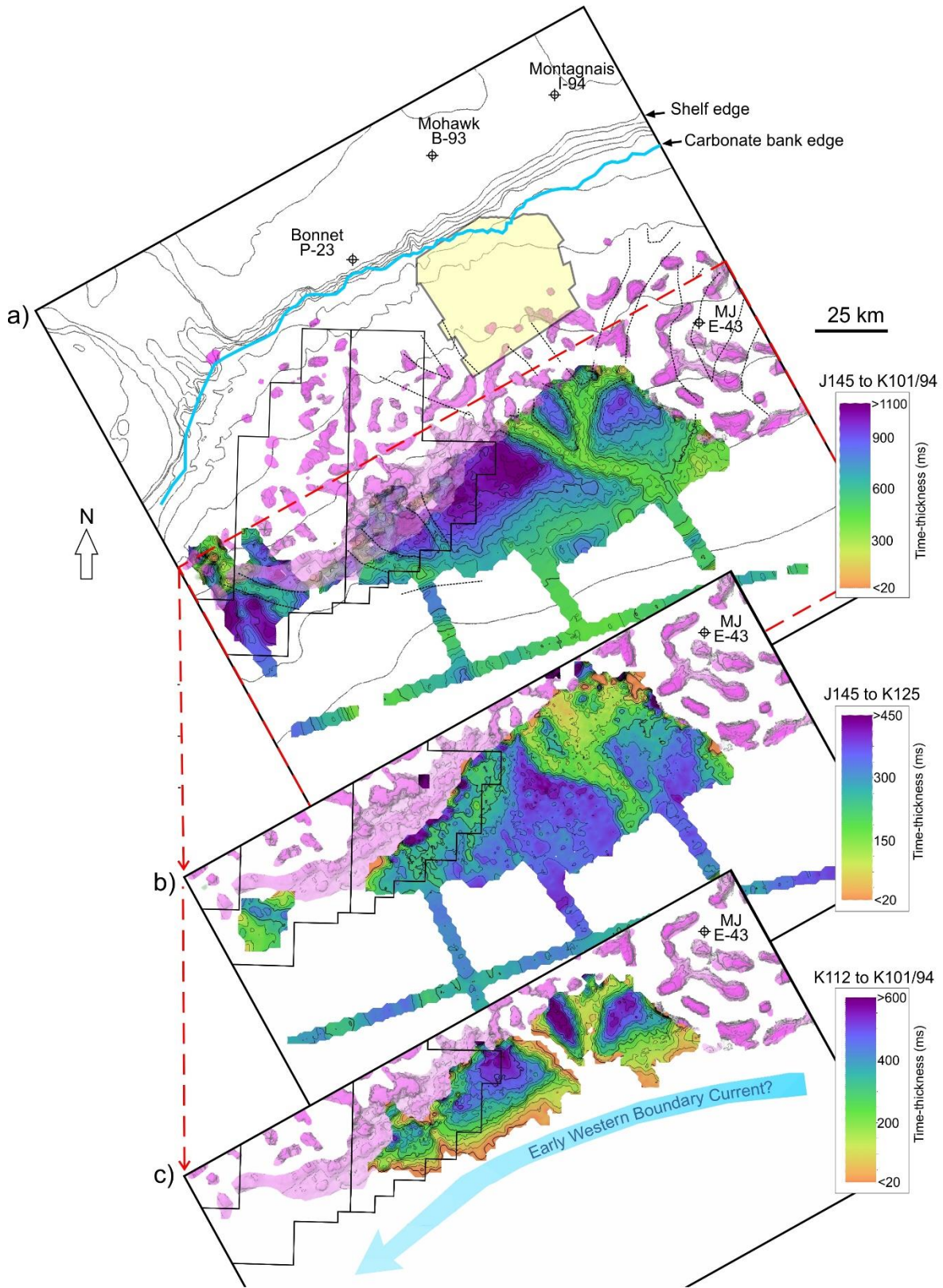
Figure 11. a) Time-thickness map between J145 and the post-K101 erosive surface showing the distribution of Lower to mid Cretaceous strata seaward of the primary salt basin. b) Time-thickness map between J145 and K125, with prominent thins corresponding to broad erosive corridors with generally higher reflection amplitudes. c) Time-thickness map between the K112 and K101 markers showing the thick low amplitude facies interpreted as a contourite drift (deeply incised from above by post-K101 canyons).

broadly forms a wedge of strata that thins abruptly seaward from ~1100 ms (twt) to less than 400 ms thick (twt) over distances of < 20 km (Figures 9, 11a). Its broad architecture resembles a contourite drift, where seismic markers merge seaward into a broad southwest-oriented scoured surface that tracks along the slope near the seaward limits of available data. In detail, however, there are also strong indications of down-slope sediment transport. As such, the entire succession is interpreted as a hybrid contourite-turbidite system, constructed by a combination of down-slope gravity-flow-dominated and cross-slope bottom-current-dominated processes (e.g. Sansom 2018; Fonnesu et al. 2019).

The architecture, lithofacies, and seismic facies distribution in Unit D is complex, made up of at least five separate sub-units (labelled **D1** to **D5**), each bound by erosional surfaces and onlapped by successive sub-units (Figures 9, 11). Thickness maps through these sub-units show a complex stacking arrangement formed during the gradual to abrupt migration of very wide (4 to 6 km) down-slope to cross-slope oriented erosional corridors that have elevated reflection amplitudes. Their adjoining lower amplitude wedge- to tabular-shaped depositional bodies show correspond gradual to abrupt shifts in sediment accumulation.

Much of the distal along-slope scouring in Figure 11a took place above the K125 marker (e.g. see Figure 11c). The faster flowing core of a southwest-flowing(?) deepwater ocean current (an early western boundary current?) is the likely candidate that removed or prevented strata from accumulating along this erosional scarp or moat (which today is located in roughly 3000 m of water). Based on its low-amplitude seismic facies, the thicker more aggradational landward parts of the drift are probably largely built of homogenous fine-grained material (Figures 9, 11c). K101 canyon incisions are anomalously deep where they cut across this feature (Figures 9a and 11a). This

probably reflects the combined effects from a period of enhanced down-slope sediment supply in the Late Albian, and focused erosion through the most topographically expressed parts of the underlying drift, as the extensive K101 canyon system attempted to establish a graded slope profile.

These canyons were largely filled by the Turonian, and overlain by an Upper Cretaceous to Lower Eocene succession dominated by pelagic chalk (**E**; Figure 9). This succession was eroded along a number of internal unconformities within Unit E, as well as the prominent T50 unconformity above Unit E that is overlain by the Montagnais mass transport depots (Deptuck and Campbell 2012). In turn, the slope seaward of the primary salt basin is overlain by the Late Eocene to Early Oligocene 'Mohawk Drift' described by Campbell and Mosher (2015).

4.   Exploration potential and uncertainties

Source rock presence

Source rock presence remains the most important exploration uncertainty off southwest Nova Scotia. As shown recently in Offshore Energy Research Association/NS Department of Energy and Mines funded studies like the 2015 SW Nova Scotia Expansion Study (OERA 2015), limited burial depths along the southwest Scotian Slope mean that source rocks younger than Middle Jurassic are unlikely to be mature. A variety of studies have attempted to demonstrate the presence of a regional Pliensbachian to Toarcian age Type II oil-prone, marine source rock interval in the Scotian Basin, including recent and ongoing piston core studies from the Scotian Slope (e.g. Fowler and Webb 2016; APT 2019a), geochemical analyses of source rocks and hydrocarbons from Morocco and Nova Scotia wells (APT 2019b), global compilations of known Lower Jurassic source rock occurrences (Bishop 2020), and seismic palinspastic reconstructions and petroleum systems modeling of the Nova Scotia-
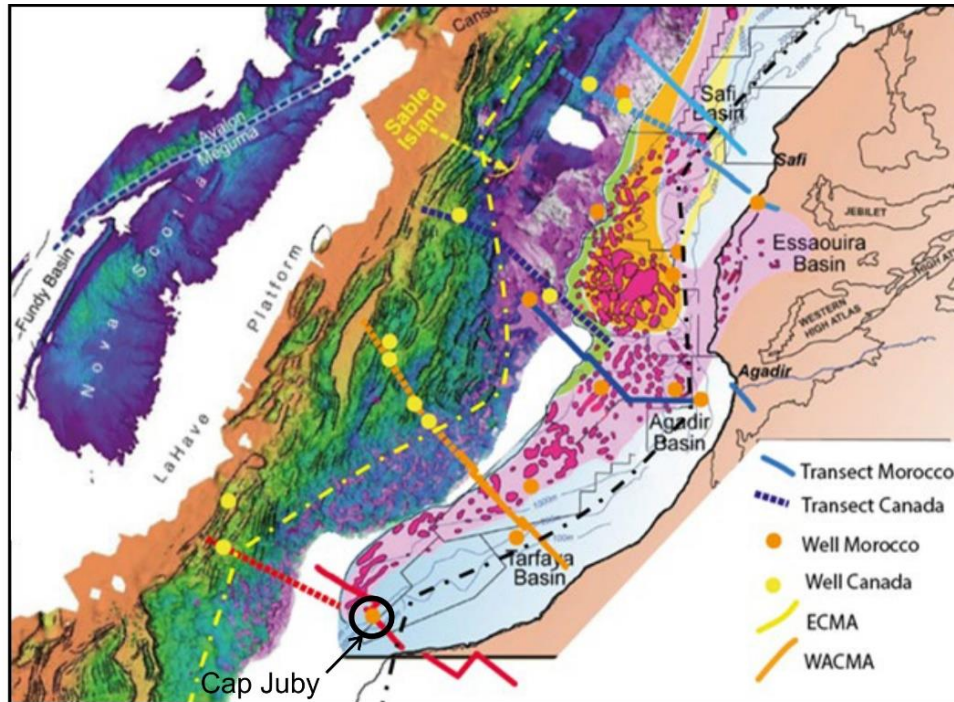
Figure 12. Plate reconstruction at 190 Ma (modified from OERA 2019). Basement map on Nova Scotia side is from Deptuck and Altheim (2018) and salt map on Moroccan side is from Tari et al. (2012). The southern part of the figure forms the matching margin pair to this study, implying this part of the Moroccan margin must also be volcanic (obscured by younger Canary Island volcanism?). The Cap Juby oil discovery in Middle to Upper Jurassic carbonates, was probably sourced from a rich Lower Jurassic marine source rock that may also exist on the southwestern Scotian margin.

Accessed in May 2020 from: https://oera.ca/research/seismic-reconstruction-and-petroleum-systems-modeling-nova-scotia-morocco-conjugate-margin

Morocco conjugate margin (OERA 2019). Of particular interest to this study are the oils in Upper to Middle Jurassic carbonate reservoirs in the Cap Juby area in the Tarfaya Basin, offshore Morocco. These oils were likely expelled from a marly Lower Jurassic restricted marine source rock (APT 2019b), and plate reconstructions indicate that this area conjugates to the West Shelburne Subbasin and Nova Scotia's volcanic margin that is the focus of this study (e.g. see location on Figure 12).

Although there is no calibration of Lower Jurassic strata off southwestern Nova Scotia, observations from reflection seismic data-sets in this study provide support for an Early Jurassic period of restricted marine sedimentation. Unit A (described earlier) forms a seaward thinning wedge of lower amplitude strata above outer domain crust (Figure 9). It aggraded landward of the SDRs as they accreted in the seaward direction, and is thickest above the earliest, inboard-most volcanic wedges. That Unit A post-dates the salt and is at least partly coeval with the SDRs, suggests it was likely deposited in the Early Jurassic. One scenario is that Unit A accumulated in a restricted shallow sea or standing lake where early thermal subsidence was
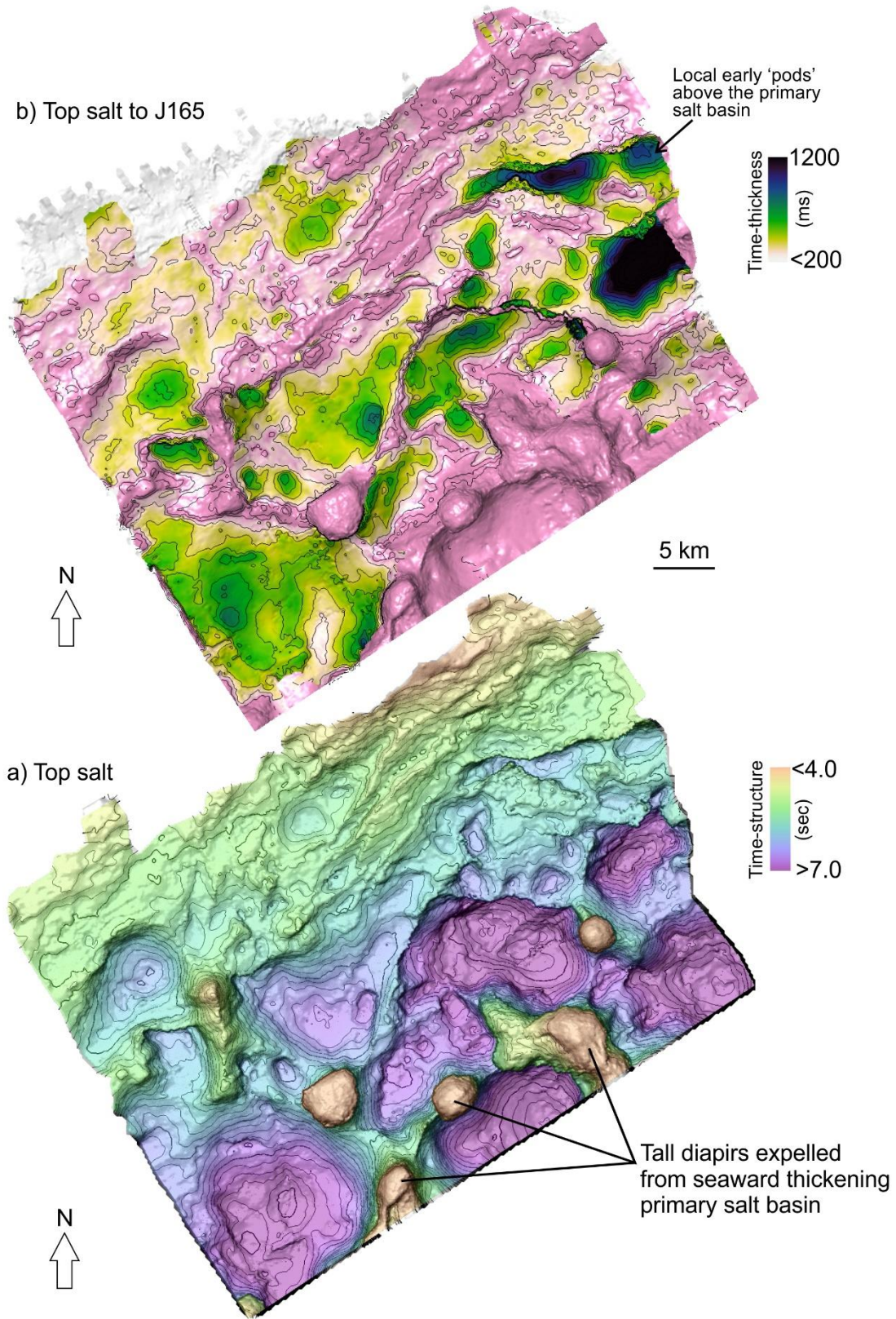
Figure 13. a) Top salt multi-z mesh from the Barrington 3D survey (contour interval is 100 ms). b) Thickness map between the top of the primary salt layer and the J165 marker, showing the distribution of earliest minibasins or rafted blocks preserved above the primary salt layer.

focused landward of the southeast accreting terrestrial volcanic wedges (Jackson et al. 2000). As the distance to the volcanic spreading centre increased, the shallow sea progressively expanded (transgressed) seaward, culminating when the spreading centre foundered and was submerged as normal oceanic crust was emplaced and an open marine environment was established. This setting may be ideal for the deposition of marly organic rich marine or lacustrine source rocks. Two widespread continuous higher amplitude soft loops within this succession (J190 marker in Figure 9) are the most likely candidates for shallow marine source rocks (troughs = reduction in acoustic impedance). Similar post-SDR depositional scenarios have been proposed for source rocks in other frontier basins (e.g. off Namibia and Argentina), and the associated seismic facies are remarkably similar (see Eastwell et al. 2018).

Lower Jurassic strata equivalent to Unit A (Figure 9) must also lie above the primary salt layer that accumulated landward, above hyperextended crust, but its distribution (and perhaps quality) will be strongly affected by salt tectonics, Early Jurassic sediment supply, and erosion (particularly approaching the necking domain). If a lower Jurassic source rock is present above the salt basin, it may be localized within early minibasins, as shown in Figure 13 from the Barrington 3D survey. Early (pre-J165) loading of the salt took place in localized depocenters that experienced a combination of detachment and rafting (mainly above thinner necking domain salt) to down-building (mainly where there was thicker salt above the landward parts of the hyperextended domain). It is not clear whether thicker Lower Jurassic depocenters favor source rock development or instead indicate a higher risk for source rock clastic dilution (e.g. see summary by Bishop 2020; CNSOPB SCOPE Atlas 2020). Although it is possible that thicker Lower Jurassic "pods" may not enhance source rock

development compared to thinner intervals, they do indicate increased preservation potential of Lower Jurassic strata, and where this interval is absent above the primary salt basin, as it is in parts of Figure 13a, so too are any associated post-salt Lower Jurassic source rocks. Aside from the Barrington 3D survey, the distribution of Lower Jurassic strata above the primary salt layer is largely unknown across much of the West Shelburne Subbasin; modern 3D seismic data is required to reconcile this.

Potential reservoirs and trap configurations

A number of potential hydrocarbon trap configurations and reservoir intervals are possible along the southwest Scotian Slope, separated into four main play concept areas (I through IV) below (Figure 14). Play concept areas mimic the distribution of crustal domains, changes in salt tectonic style, and water depth.

Play concept area I (**PCA I**; Figure 14) is located along the seaward boundary of the proximal domain, along the margin hinge. Here, PCA I forms a narrow band that in Figure 14 covers a roughly 100 km long reach of the Upper Jurassic carbonate bank edge where there is potential for porous reef margin reservoirs. The play concept is essentially that of the Deep Panuke gas field along the margins of the Sable Subbasin (Kidston et al. 2005). Although production of gas in the Deep Panuke field proved challenging due to excess water production, liquid hydrocarbons would pose fewer production issues. Bonnet P-23 tested this region 36 years ago, but the well was located about 6 km inboard of the bank edge and targeted porous Jurassic siliciclastic reservoirs that had been identified 14 years earlier still at Mohawk B-93. No reef-related facies were encountered. New 3D seismic data are required to properly identify and evaluate leads associated with reef margin reservoirs, and to assess top seal (as Cretaceous to early Paleogene erosion was focused above the bank edge and there is a risk that traps in this setting could be breached).
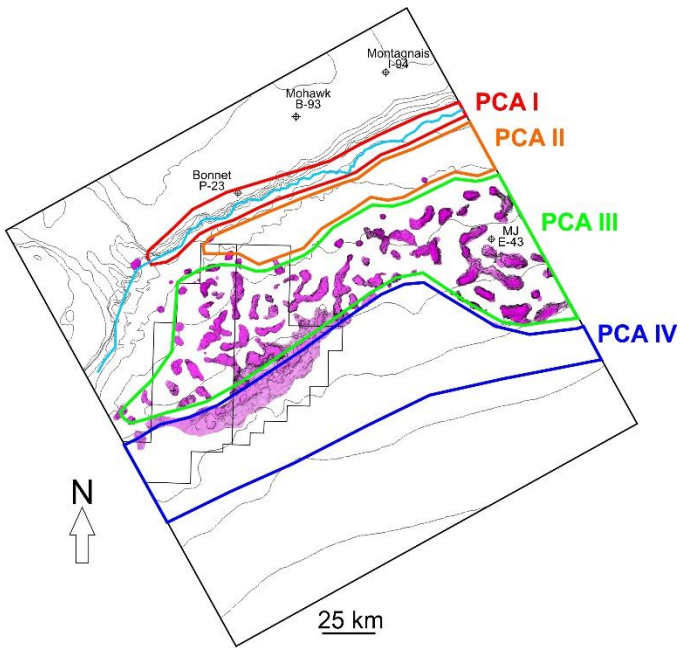
Figure 14. Play concept areas (PCA) along the southwestern Scotian margin.

Further seaward, play concept area II (**PCA II**; Figure 14) comprises a number of potential structural traps below the primary salt layer (e.g. Figure 15) and stratigraphic traps above the primary salt layer. PCA II is underpinned by necking domain crust that is overlain by pre-salt synrift strata, in turn covered by the landward thinning margin of the primary salt basin. Salt has variously been welded out or deformed into pillows and rollers, or preserved as thicker remnants along graben axes. There are no tall salt diapirs in PCA II, and the area is equivalent to the "slope detachment province" described in Deptuck (2011).

Like rift basins above the LaHave Platform further east (e.g. Deptuck and Altheim 2018), the layered stratigraphic succession *below* the primary salt layer is heavily faulted (Figures 6a, 15), and there is potential for a number of fault-dependent traps all along the necking domain. For example, the Muskat lead in Figure 15 is a ~20 km^2 three-way fault-dependent closure along the top presalt/base salt surface in the Barrington 3D volume. The crest of the structure is relatively shallow, at a subsea depth

of roughly 6 km (Figure 15). The composition of the presalt succession is unknown, but reservoirs could comprise synrift amalgamated fluvial channel bodies like the ones encountered on the LaHave Platform at Sambro I-29 (Deptuck and Altheim 2018). Although these traps underlie the primary salt layer, in the Muskat lead, the overlying salt layer is very thin or welded out, which could increase trap integrity risk. A thin or absent salt seal, however, may also allow lower Jurassic source rocks to expel hydrocarbons into older synrift reservoirs, eliminating the need for a pre-salt source rock.

A number of potential stratigraphic traps are also possible *above* the primary salt layer in PCA II, involving Cretaceous to early Paleogene turbidite reservoirs that onlap the steep low-accommodation carbonate foreslope (e.g. Figures 16, 17). Numerous amplitude anomalies terminate both up-dip and down-dip, and conform to structure (see figure 2.21 of Deptuck et al. 2015). For example, two main intervals in the Barrington 3D survey produce anomalous amplitudes (Figure 16). Amplitude extractions from the lower interval (~K94 marker) show a clear network of channels converging down-slope into trunk channels, with an abrupt downslope amplitude cut-off (Figure 17b). The shallower interval (T50 to K85) is broader, with less clearly defined channels but shows a similar amplitude cut-off (Figure 17c). They are interpreted to correspond to turbidite channel reservoirs contained within a combination up-slope pinch-out and angular unconformity trap (Figure 16a). Their up-dip termination is associated with onlap onto the carbonate foreslope and, more important, erosion along the T50 unconformity that was later draped by widespread Late Eocene mudstones (Cayuga lead described by Deptuck et al. 2015). They are underlain by variably thick "pods" of Lower Jurassic strata, with numerous faults providing charge access (Figure 17a).
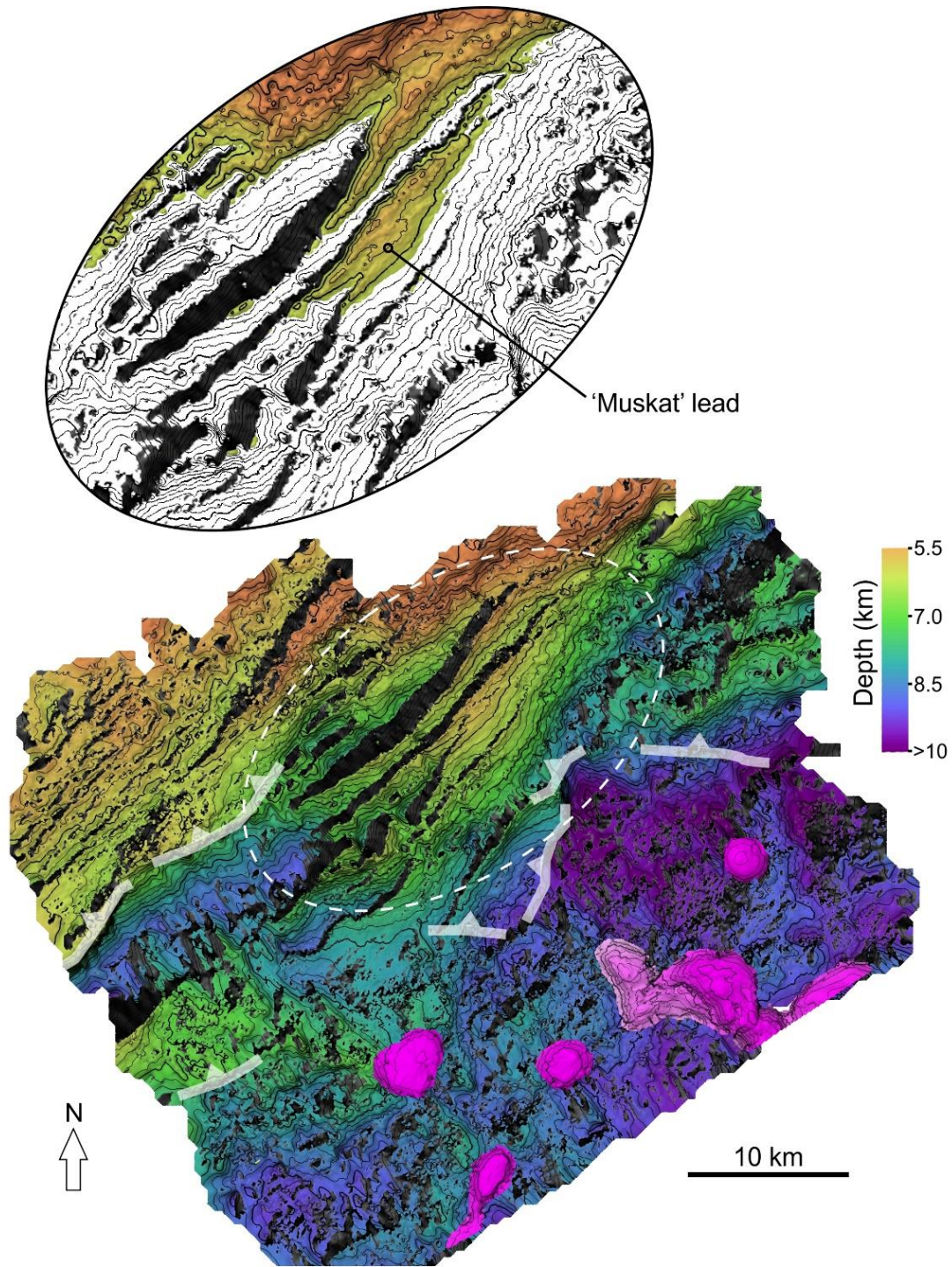
Figure 15. Depth-structure map along the heavily faulted base-salt surface, from the Barrington 3D seismic volume. Most faults are extensional and dip towards the northwest. A number of faults appear to have experienced some inversion after the primary salt layer was deposited (identified in white). Taller salt diapirs identified in pink. Inset shows the Muskat lead, a potential pre-salt structural trap with 20 km^2 of fault-depended closure. Depth conversion based on a simple four-layer velocity model. Contour interval is 200 m. See Figures 3 for location and 6a for a representative section across the faulted pre-salt succession.

The vertical stacking of these anomalies (and maybe even deeper presalt leads like Muskat; Figure 17a), their very large aerial coverage (>250 km^2 just within the Barrington 3D survey; Deptuck et al. 2015), relatively shallow burial depths, and relatively shallow present day water depths (<1500 m), make them potentially attractive targets. However, their position above a low accommodation mainly bypass slope means they could form narrow, thin, and complex ribbon-like reservoir elements (e.g. Prather 2020). It is also possible that the anomalies are produced by high impedance fill within channels (perhaps resedimented carbonates eroded from the carbonate bank?) or tuning effects, and as such the source of these amplitude anomalies requires further study. Similar anomalies are recognized on the slope both west and east of the Barrington 3D survey (Figure 10), so they are not unique to the processing workflow specific to any one survey. Likewise, there are also a number of amplitude anomalies involving Miocene and Pliocene turbidite or even sandy contourite reservoirs that pinch-out into potential stratigraphic traps along a regional Miocene onlap surface; these too require further investigation.

Further seaward still, in play concept area III (**PCA III**; Figure 14), there are a number of leads associated with potential turbidite reservoirs that onlap or drape salt diapirs (folds above salt bodies or three way traps on salt diapir flanks). The sharp increase in prominent salt diapirs (mainly vertical walls and stocks) in PCA III reflects the increased thickness of the primary salt layer above hyperextended crust. Jurassic, Cretaceous, and Cenozoic minibasins developed through sustained, mainly vertical, down-building into the primary salt layer. There are also clear indications of thin-skinned(?) shortening within in PCA III, down-slope from regions of thin-skinned extension (e.g. Figure 8d), with resulting folds forming potential traps within minibasins (e.g. figure 10c of Deptuck and Kendell 2017). Most

diapirs in PCA III were reactivated and squeezed during the Cenozoic, and so folds involving Cretaceous and Cenozoic strata are commonly localized above isolated salt bodies (Figure 16).

A number of potential direct hydrocarbon indicators, like bright spots and other seismic anomalies, have been identified in PCA III (e.g. see Hall and Bianco 2016). They are recognized both at shallow intervals that likely correspond to Bottom Simulating Reflectors (BSRs) associated with gas hydrates (typically within 500 ms twt of the seabed; e.g. green arrows in Figure 16), and at deeper intervals that clearly conform to structure above or on the flanks of squeezed salt diapirs (e.g. Figures 16c, 17c).

In Jurassic and Cretaceous intervals, the erosive floors of some channels/canyons correspond to one or more bright amplitude reflections, produced by the impedance contrast between the basal incision surface and underlying pre-canyon strata, or the impedance contrast between lower (coarser grained?) and upper (finer grained?) canyon fill. In the latter scenario, coarse grained material above canyon floors could form viable reservoirs, though reservoir quality in this setting is unclear. Some canyon axes do appear to be up on structure, particularly where they have transited underlying salt bodies that were later squeezed, in some cases with diapirs piercing wide canyon floors (e.g. Figure 8b, c). This study shows that some canyon systems, for example at the K125, K101 and T50 markers, are anomalously wide and erosive, both removing wide swaths of slope strata and restricting the accumulation of any potential reservoirs to their floors or areas seaward of PCA III (see CNSOPB SCOPE Atlas, 2020). To identify reservoirs outside canyon axes in PCA III, a detailed analysis of the evolution of turbidite corridors and sediment partitioning on the slope is required. Some of the smaller channel systems probably deposited sand prone slope aprons within some minibasins, for
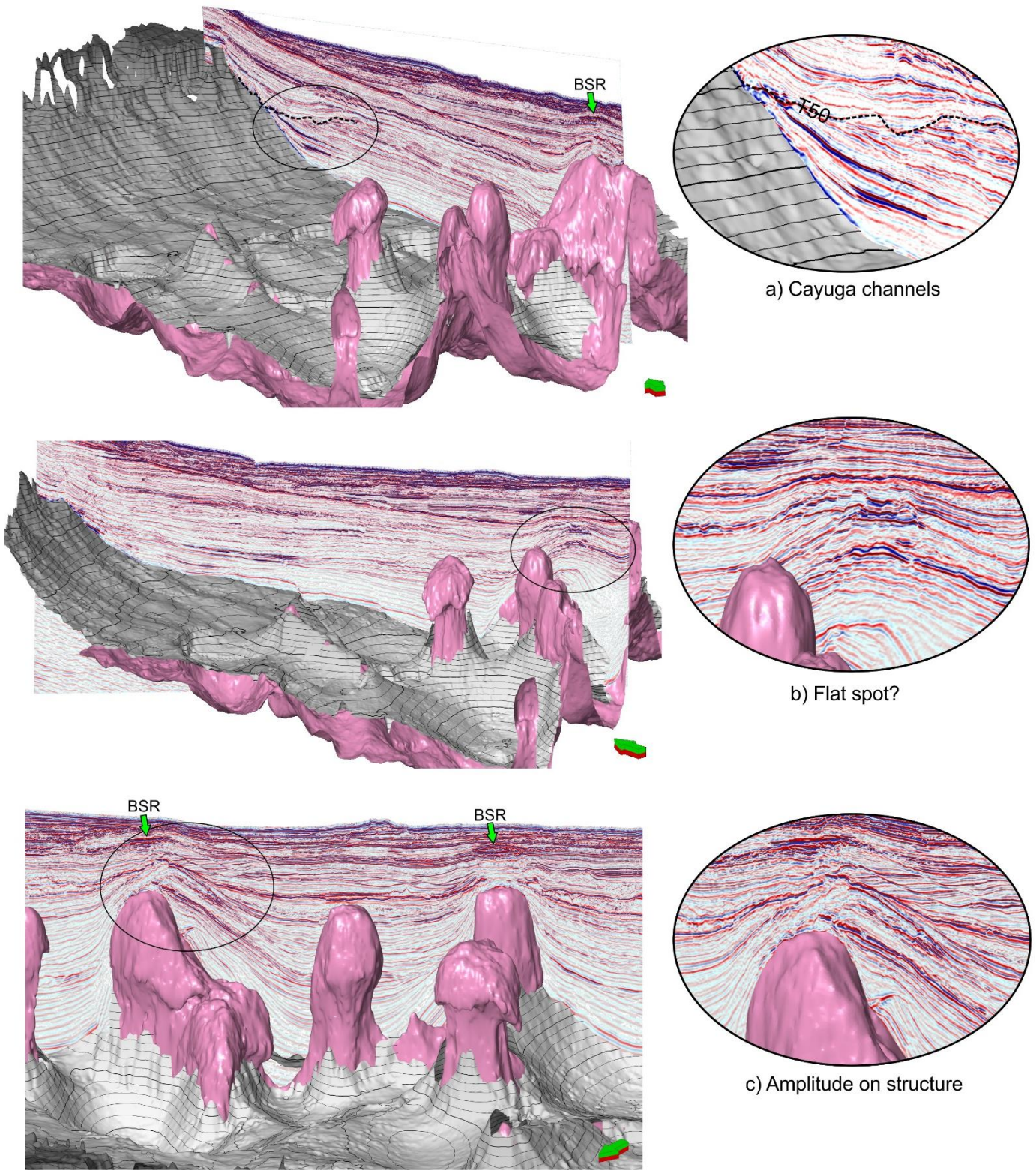
a) Cayuga channels

b) Flat spot?

c) Amplitude on structure

Figure 16. Perspective view examples of potential DHIs in the Barrington 3D seismic volume, onlapping the steep carbonate foreslope in play concept area II, and found above or on the flanks of salt structures in play concept area III. Grey contoured surface is the J145 marker; salt diapirs are shown in pink.

example in the seaward parts of the Barrington 3D volume in Figure 17b, but careful study is required to distinguish true slope aprons from the very wide floors of some canyons.

Play concept area IV (**PCA IV**; Figure 14) is located seaward of the primary salt basin, but with some influence from overhanging salt bodies that were expelled up and over Jurassic strata and underlying SDRs. The complex stratigraphy in this region (described earlier) directly overlies Unit A - the probable Lower Jurassic interval with candidate source rocks. Reservoirs are likely to be restricted to the very broad (>3 km wide) canyon floors or fairway corridors that, along with their more elevated margins, migrated and stacked in complex ways seaward of the salt basin. In some cases progressive lateral migration of broad reservoir-prone corridors produced more extensive accumulations of interpreted coarser grained material (a number of these corridors are shown in Figure 10), bordered by thicker finer grained off-axis sediment accumulations (levees or drifts, or some combination).

Most traps are likely to be stratigraphic, but may include a structural component where reservoir elements pinch-out above salt bodies in the landward most part of PCA IV. For example, one wide potential reservoir body was deposited along a corridor that runs parallel to the seaward pinch-out of the Shelburne salt tongue (the *Petite Pearl* lead; Figures 10 inset). It corresponds to a single 3.5 to 8 km wide bright reflection correlated more than 60 km along-strike and covering an area of ~270 km^2. It is largely located in Equinor acreage, but also extends east where a number of other similar features are also found (Figure 10).

As described earlier, the succession between K125 and K94, in particular, is interpreted to have formed through the complex interaction of down-slope and cross-slope processes (a hybrid contourite-turbidite system). In the seaward parts of the study area especially, the Cretaceous systems are closely similar to hybrid systems described in Tanzania and Mozambique that can be associated with thick, clean sandstone reservoirs, and in some cases giant hydrocarbon accumulations (like the super-giant ~80 TCF Coral and Mamba gas fields in the offshore of Northern Mozambique prolific (Sansome 2018; Fonessu et al. 2019).

Finally, it is possible that the J165 to J145 higher-amplitude, complex seismic facies located seaward of the primary salt basin has reservoir potential. The succession ultimately underlies salt overhangs of the Shelburne salt tongue/canopy and more isolated salt overhangs to its east. These could form large traps. Broad folds are also recognized in strata above some SDRs on time-migrate seismic profiles (e.g. Figure 9b), that could form equally large traps if the folds still exist on depth migrated profiles.

Recommended citation
Deptuck, M.E (2020) Nova Scotia's volcanic passive margin - exploration history, geology, and play concepts off southwestern Nova Scotia. CNSOPB Geoscience Open File Report 2020-001MF, 32 p.
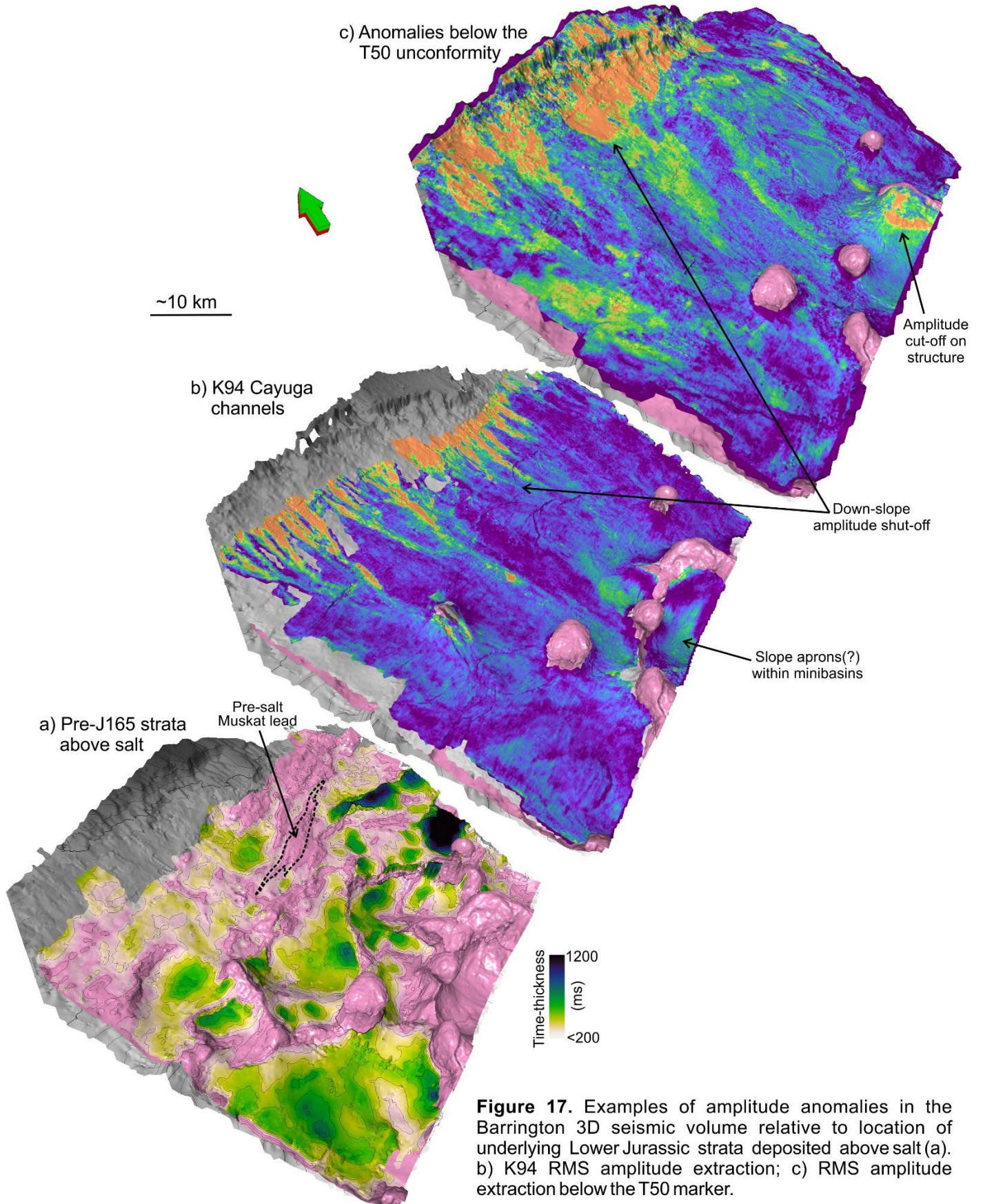
c) Anomalies below the T50 unconformity

~10 km

b) K94 Cayuga channels

Amplitude cut-off on structure

Down-slope amplitude shut-off

Slope aprons(?) within minibasins

Pre-salt Muskat lead

a) Pre-J165 strata above salt

Time-thickness (ms)
1200
<200

Figure 17. Examples of amplitude anomalies in the Barrington 3D seismic volume relative to location of underlying Lower Jurassic strata deposited above salt (a). b) K94 RMS amplitude extraction; c) RMS amplitude extraction below the T50 marker.

29

References

Allen, J. and Beaumont, C. (2015) Continental margin syn-rift salt tectonics at intermediate width margins, Basin Research, p. 1–36, doi: 10.1111/bre.12123

Allen, J., Beaumont, C. and Deptuck, M.E. (2019) Feedback between syn-rift lithospheric extension, sedimentation, and salt tectonics on wide, weak continental margins, Petroleum Geoscience, 26: 16-35

APT (2019a) Geochemistry Data Report for 2018 Scotian Slope Coring Program. Report APT-18-5348. 308 p. https://oera.ca/research/piston-coring-geochemistry-program (file downloaded May 2020)

APT (2019b) Jurassic Oils and Source Rocks of Northern Morocco, 347 p. https://oera.ca/research/2018-nova-scotia-morocco-conjugate-geochemistry-project (file made available from the Offshore Energy Research Association in May 2020)

Austin, J.A., Stoffa, P.L., Phillips, J.D., Oh, J., Sawyer, D.S., Purdy, G.M., Reiter, E., and Makris, J. (1990) Crustal structure of the Southeast Georgia embayment-Carolina trough: Preliminary results of a composite seismic image of a continental suture(?) and a volcanic passive margin, Geology, 18: 1023–1027

Biari, Y., Klingelhoefer, F., Sahabi, M., Funck, T., et al. (2017) Opening of the central Atlantic Ocean: Implications for geometric rifting and asymmetric initial seafloor spreading after continental breakup, Tectonics, 36: 1129-1150

Bishop, A.N. (2020) Greater North Atlantic Liassic Petroleum Systems Synthesis, Technical Report OG-2020-01 https://oera.ca/research/greater-north-atlantic-liassic-petroleum-systems-synthesis (file downloaded in May 2020)

Campbell, D.C. and Deptuck, M.E. (2012) Alternating bottom current dominated and gravity flow dominated deposition in a lower slope and rise setting – insights from the seismic geomorphology of the western Scotian margin, Eastern Canada, In: B. Prather, M. Deptuck, D. Mohrig, B. van Hoorn, and R. Wynn (Eds), Application of the Principles of Seismic Geomorphology to Continental Slope and Base-of-slope Systems: Case Studies from Seafloor and Near-Seafloor Analogues, SEPM Special Publication 99, p. 329-346

Campbell, D.C., Shimeld, J., Deptuck, M.E., Mosher, D.C. (2015) Seismic stratigraphic framework and depositional history of a large Upper Cretaceous and Cenozoic depocenter off southwest Nova Scotia, Canada. Marine and Petroleum Geology, 65: 22–42

Campbell, D.C., and Mosher, D.C. (2015) Geophysical evidence for widespread Cenozoic bottom current activity from the continental margin of Nova Scotia, Canada, Marine Geology, 378: 237-260

Chenin, P., Manatschal, G., Picazo, S., Muntener, O., Karner, G., Johnson, C., and Ulrich, M. (2017) Influence of the architecture of magma-poor hyperextended rifted margin on orogens produced by the closure of narrow versus wide oceans, Geosphere, 13: 559-576

CNSOPB SCOPE Atlas (2020) Atlas of 3D seismic surfaces and thickness maps, central to western Scotian Slope. Available July 2020 here: https://www.cnsopb.ns.ca/what-we-do/resource-management/geoscience-publications

Dehler, S.A., Keen, C.E., Funck, T., Jackson, H. R. & Louden, K.E. (2004) The limit of volcanic rifting: A structural model across the volcanic to non-volcanic transition off Nova Scotia. Eos Trans. AGU, 85(17), Jt. Assem. Suppl., Abstract T31D-04.

Dehler, S.A. (2012) Initial rifting and breakup between Nova Scotia and Morocco: insight from new magnetic models, Canadian Journal of Earth Sciences, 49: 1395-1415

Deptuck, M.E. (2011) Proximal to distal postrift structural provinces on the western Scotian Margin, offshore Eastern Canada: Geological context and parcel prospectivity for Call-for-Bids NS11-1, Canada-Nova Scotia Offshore Petroleum Board, Geoscience Open File Report (GOFR) 2011-001MF, 42p. Available here: https://www.cnsopb.ns.ca/what-we-do/resource-management/geoscience-publications

Deptuck, M.E. and Campbell, D.C. (2012) Widespread erosion and mass failure from the ~51 Ma Montagnais marine bolide impact off southwestern Nova Scotia, Canada, Canadian Journal of Earth Sciences, 49: 1567-1594

Deptuck, M.E., Brown, D.E. and Altheim, B. (2015) Call for Bids NS15-1 – Exploration history, geologic setting, and exploration potential: Western and Central regions. CNSOPB Geoscience Open File Report 2015-001MF, 49 p. Available here: https://www.cnsopb.ns.ca/what-we-do/resource-management/geoscience-publications

Deptuck, M.E. and Kendell, K.L. (2017) Chapter 13: A review of Mesozoic salt tectonics along the Scotian margin, eastern Canada, In: J. Soto, J. Flinch, and G. Tari, (Eds), Permo-Triassic Salt Provinces of Europe, North Africa and Central Atlantic: Tectonics and Hydrocarbon Potential, Elsevier, p. 287-312

Deptuck, M.E. and Altheim, B. (2018) Rift basins of the central LaHave Platform, offshore Nova Scotia. CNSOPB Geoscience Open File Report 2018-001MF, 54 p. Available here: https://www.cnsopb.ns.ca/what-we-do/resource-management/geoscience-publications

Deptuck, M.E. (2018) Insights into crustal structure and rift basin development off central and western Nova Scotia – a

reflection seismic perspective, Conjugate Margins Conference, Halifax, Nova Scotia, Atlantic Geology, 54: 421

Eastwell, D., Hodgson, N., and Rodriguez, K. (2018) Source rock characterization in frontier basins – a global approach, First Break, 36: 3-10

Fensome, R.A., Crux, J.A., Gard, I.G., MacRae, R.A., Williams, G.L., Thomas, F.C., Fiorini, F., and Wach, G. (2008) The last 100 million years on the Scotian Margin, offshore eastern Canada: an event-stratigraphic scheme emphasizing biostratigraphic data. Atlantic Geology, 44: 93-126

Fonnesu, M., Palermob, D., Galbiatia, M., Marchesinia, M., Bonaminia, E., and Bendiasc, D. (2019) A new world-class deep-water play-type, deposited by the syndepositional interaction of turbidity flows and bottom currents: The giant Eocene Coral Field in northern Mozambique, Marine Petroleum Geology, 111: 179-201

Fowler, M. and Webb, J. (2016) Geochemistry Data Report for 2016 Scotian Slope Piston Coring Program, 620 p. (Report downloaded in April 2020 from https://oera.ca/research/piston-coring-geochemistry-program)

Franke, D. (2012) Rifting, lithosphere breakup and volcanism: Comparison of magma-poor and volcanic rifted margins: Marine Petroleum Geology, 43: 63–87

Geoffroy, L., Burov, E.B., and Werner, P. (2015) Volcanic passive margins: another way to break up continents: Nature, Scientific Reports, 5: 14828

Hall, M., and Bianco, E. (2016) Direct hydrocarbon indicator mapping, offshore Nova Scotia [Project 400111], 13 p. (Report downloaded in April 2020 from https://oera.ca/research/direct-hydrocarbon-indicator-dhi-mapping-offshore-nova-scotia)

Hanford, C.R., and Baria, L.R. (2007) Geometry and seismic geomorphology of carbonate shoreface clinoforms, Jurassic Smackover Formation, north Louisiana, in R.J. Davies, H.W. Posamentier, L.J. Wood, and J.A. Cartwright (Eds), Seismic Geomorphology: Applications to Hydrocarbon Exploration and Production, Geological Society of London, 277: 171-185

Jansa, L.F., and Pe-Piper, G. (1987) Identification of an underwater extraterrestrial impact crater. Nature, 327: 612-614

Jansa, L.F., Pe-Piper, G., Robertson, P.B., and Freidenreich, O. (1989) Montagnais: A submarine impact structure on the Scotian Shelf, eastern Canada. GSA Bulletin, 101: 450-463

Jackson, M.P.A., Cramez, C., and Fonck, J-M. (2000) Role of subaerial volcanic rocks and mantle plumes in creation of South Atlantic margins: implications for salt tectonics and source rocks, Marine and Petroleum Geology, 17: 477-498

Keen, C.E. and Potter, D.P. (1995) Formation and evolution of the Nova Scotia rifted margin: Evidence from deep seismic reflection data, Tectonics, 14: 918-932

Keen, C.E. and Potter, D.P. (1995) The transition from a volcanic to nonvolcanic rifted margin off eastern Canada. Tectonics, 14: 359-371

Kidston, A.G., Brown, D.E., Smith, B.M., and Altheim, B. (2005) The Upper Jurassic Abenaki Formation, offshore Nova Scotia: A seismic and geologic perspective, Canada Nova Scotia Offshore Petroleum Board, Halifax, Nova Scotia, 168 p. Available here: https://www.cnsopb.ns.ca/what-we-do/resource-management/geoscience-publications

Louden, K., Wu, Y. and Tari, G. C. (2012) Systemic variations in basement morphology and rifting geometry along the Nova Scotia and Morocco conjugate margins, In W . U. Mohriak, A. Danforth, P. J. Post, D. E. Brown, G. C. Tari, M. Nemčok & S. T. Sinha, (Eds.), Conjugate Divergent Margins. Geological Society of London Special Publications, 369: 267-287

Moscardelli, L. Ochoa, J., Lunt, I., and Zahm, L. (2019) Mixed siliciclastic–carbonate systems and their impact for the development of deep-water turbidites in continental margins: A case study from the Late Jurassic to Early Cretaceous Shelburne subbasin in offshore Nova Scotia, AAPG Bulletin, 103: 2487-2520

McDermott, K., Gillbard, E., and Clarke, N. (2015) From basalt to skeletons - the 200 million-year history of the Namibian margin uncovered by new seismic data: First Break, 33: 77-85.

Mutter, J.C., Talwani, M., Stoffa, P.L., 1982. Origin of seaward-dipping reflectors in oceanic crust off the Norwegian margin by "subaerial sea-floor spreading", Geology, 10: 353-357

OERA (2015) South West Nova Scotia Expansion: Georges Bank and Shelburne Subbasin Study. Nova Scotia Department of Energy Report. https://oera.ca/research/sw-nova-scotia-expansion-atlas-2015

OERA (2019) Seismic reconstruction, thermal and maturity modeling of Nova Scotia and northern Morocco conjugate margins; https://oera.ca/research/seismic-reconstruction-and-petroleum-systems-modeling-nova-scotia-morocco-conjugate-margin downloaded May 2020

OETR (2011) Play Fairway Analysis Atlas - Offshore Nova Scotia, Nova Scotia Department of Energy Report, NSDOE Records Storage File No. 88-11-0004-01, 347p. https://oera.ca/research/play-fairway-analysis-atlas

Oh, J., Austin, J. A., Phillips, J. D., Coffin, M. F., and Stoffa, P. L. (1995) Seaward-dipping reflectors offshore the southeastern

United States: Seismic evidence for extensive volcanism accompanying sequential formation of the Carolina trough and Blake plateau basin, Geology, 23: 9–12

Paton, D.A., Pindell, J., McDermott, K., Bellingham, P., Horn, B. (2017) Evolution of Seaward Dipping Reflections at the onset of oceanic crust formation, Geology, 45: 439-442

Pe-Piper, G. and Jansa, L.F. (1999) Pre-Mesozoic basement rocks offshore Nova Scotia, Canada: new constraints on the origin and Paleozoic accretionary history of the Meguma terrane, Bulletin of the Geological Society of America, 111: 1773-1791

Peron-Pinvidic, G., Manatschal, G., Osmundsen (2013) Structural comparison of archetypal Atlantic rifted margins: A review of observations and concepts, Marine and Petroleum Geology, 43: 21-47

Pindell, J., Graham, R., and Horn, B. (2014) Rapid outer marginal collapse at the rift to drift transition of passive margin evolution, with a Gulf of Mexico case study: Basin Research, 26: 701–725

Planke S., Symonds P., Alvestad E., and Skogseid J. (2000) Seismic volcanostratigraphy of large-volume basaltic extrusive complexes on rifted margins: Journal of Geophysical Research, 105: 19335–19351

Prather, B. (2020) Controls on Reservoir Distribution, Architecture and Stratigraphic Trapping in Slope Settings, in N. Scarselli, J. Adamand, D. Chiarella (Eds), Regional geology and tectonics (2nd ed.), Volume 1: Principles of geologic analysis, Elsevier B. V. doi: https://doi.org/10.1016/B978-0-444-64134-2.00025-0

Reuber, K. Mann, P., and Pindell, J. (2019) Hotspot origin for asymmetrical conjugate volcanic margins of the austral South Atlantic Ocean as imaged on deeply penetrating seismic reflections lines, Interpretation, 7: 71-97

Rowan, M.G. (2014) Passive-margin salt basins: hyperextension, evaporate deposition, and salt tectonics. Basin Research, 26: 154–182

Ross, W.C., Halliwell, B.A., May, J.A., Watts, D.E., and Syvitski, J.P.M. (1994) Slope readjustment: a new model for the development of submarine fans and aprons: Geology, 22: 511-514

Sansom, P. (2018) Hybrid turbidite-contourite systems of the Tanzanian margin, Petroleum Geoscience, 24: 258-276

Shimeld, J. (2004) A comparison of salt tectonic subprovinces beneath the Scotian Slope and Laurentian Fan. In: P.J. Post, D.L. Olsen, K.T. Lyons, S.L. Palmes, P.F. Harrison, and N.C. Rosen (Eds) Salt-Sediment Interactions and Hydrocarbon Prospectivity: Concepts, Applications, and Case Studies for the 21st Century, 24th Annual GCS-SEPM Foundation Bob F. Perkins Research Conference, Houston, p.502-532, CD-ROM

Sutra, E. Manatschal, G., Mohn, G., and Unternehr, P. (2013) Quantification and restoration of extensional deformation along the Western Iberia and Newfoundland rifted margins, AGU Geochemistry Geophysics Geosystems, 14: 2575-2597

Tari, G., Brown, D., Jabour, H., Hafid, M., Louden, K. & Zizi, M. (2012) The conjugate margins of Morocco and Nova Scotia. In D.G. Roberts & A.W. Bally (Eds.) Regional Geology and Tectonics: Phanerozoic Passive Margins, Cratonic Basins and Global Tectonic Maps, Amsterdam: Elsevier, p.285–323.

Wade, J.A. and MacLean, B.C. (1990) The geology of the Southeastern Margin of Canada, Chapter 5, In M.J. Keen and G.L. Williams (Eds), Geology of the Continental Margin of Eastern Canada, Geological Survey of Canada, The Geology of Canada, p. 224-225

Welsink., H.J., Dwyer, J.D. and Knight, R.J. (1989) Tectono-stratigraphy of the passive margin off Nova Scotia, Chapter 14, In: A.J. Tankard and H.R. Balkwill (Eds) Extensional Tectonics and Stratigraphy of the North Atlantic Margins, AAPG Memoir 46: 215-231

Weston, J.F., MacRae, R.A., Ascoli, P., Cooper, M.K.E., Fensome, R.A., Shaw, D. and Williams, G.L. (2012) A revised biostratigraphic and well-log sequence stratigraphic framework for the Scotian Margin, offshore eastern Canada, Canadian Journal of Earth Sciences, 49: 1417-1462

Wu, Y., Louden, K. E., Funck, T., Jackson, H. R. & Dehler, S. A. (2006) Crustal structure of the central Nova Scotia margin off Eastern Canada. Geophysical Journal International, 166: 878-90